

Discovery of a Series of Potent, Selective, and Orally Bioavailable Nucleoside Inhibitors of CD73 That Demonstrates *In Vivo* Antitumor Activity

Jim Li,* Lijing Chen, Roland J. Billedeau, Timothy F. Stanton, John T. P. Chiang, Clarissa C. Lee, Weiqun Li, Susanne Steggerda, Ethan Emberley, Matthew Gross, Deepthi Bhupathi, Xiaoying Che, Jason Chen, Rosalyn Dang, Tony Huang, Yong Ma, Andrew MacKinnon, Amani Makkouk, Gisele Marguier, Silinda Neou, Natalija Sotirovska, Sandra Spurlock, Jing Zhang, Winter Zhang, Michael van Zandt, Lin Yuan, Jennifer Savoy, Francesco Parlati, and Eric B. Sjogren*



Cite This: *J. Med. Chem.* 2023, 66, 345–370



Read Online

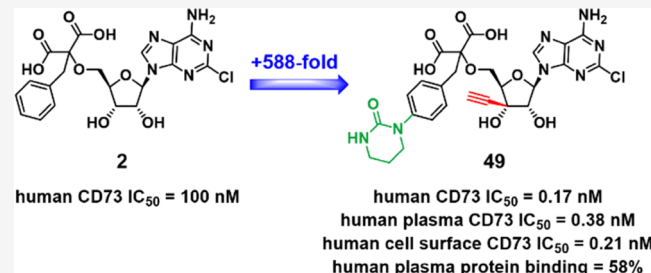
ACCESS |

Metrics & More

Article Recommendations

Supporting Information

ABSTRACT: CD73 (ecto-5'-nucleotidase) has emerged as an attractive target for cancer immunotherapy of many cancers. CD73 catalyzes the hydrolysis of adenosine monophosphate (AMP) into highly immunosuppressive adenosine that plays a critical role in tumor progression. Herein, we report our efforts in developing orally bioavailable and highly potent small-molecule CD73 inhibitors from the reported hit molecule **2** to lead molecule **20** and then finally to compound **49**. Compound **49** was able to reverse AMP-mediated suppression of CD8⁺ T cells and completely inhibited CD73 activity in serum samples from various cancer patients. In preclinical *in vivo* studies, orally administered **49** showed a robust dose-dependent pharmacokinetic/pharmacodynamic (PK/PD) relationship that correlated with efficacy. Compound **49** also demonstrated the expected immune-mediated antitumor mechanism of action and was efficacious upon oral administration not only as a single agent but also in combination with either chemotherapeutics or checkpoint inhibitor in the mouse tumor model.



INTRODUCTION

T cells play a critical role in controlling the onset and progression of cancer, but a range of potent immunosuppressive mechanisms can be upregulated in the tumor microenvironment (TME) to abrogate their activity.^{1,2} The development of immunotherapies targeted at re-invigorating the T-cell-mediated antitumor response, such as immune checkpoint blockade and adoptive cell transfer (ACT) of tumor-specific T cells, has led to unparalleled clinical responses in recent years.³ To extend the benefit of immunotherapy to a broader range of cancers, targeting additional mechanisms of tumor immune evasion will be critical.^{4–6} Extracellular adenosine (ADO) signaling has emerged as a key metabolic pathway that regulates tumor immunity. ADO inhibits the cytotoxic and effector functions of T cells and NK cells and induces immunosuppressive cell types, such as Tregs, MDSCs, TAMs, and tolerogenic DCs, and enhances their functions via binding to A2A and A2B receptors.^{7–11} Extracellular ADO can be produced from adenosine triphosphate (ATP) that is released during cell death or stress through the sequential activity of ectonucleotidases CD39 (NTPDase 1) and CD73 (ecto-5'-nucleotidase or NTSE). In the adenosinergic pathway, CD39 dephosphorylates ATP to adenosine monophosphate

(AMP), while CD73 catalyzes the final step of hydrolyzing AMP to adenosine and inorganic phosphate (Figure 1).^{12–14} Both CD39 and CD73 are highly expressed on tumor cells and cancer cell-derived exosomes within the TME.^{15,16} High CD73 expression in multiple tumor tissues has been correlated to unfavorable clinical outcomes, such as poor overall prognosis and survival, high metastasis, and chemoresistance.^{17–25}

CD73 is a homodimer that is attached to the outer leaflet of the plasma membrane via a glycosylphosphatidylinositol (GPI)-anchor.²⁵ Cleavage of the GPI-anchor by phospholipase C releases a soluble form that exhibits similar enzymatic activity. Hydrolysis of AMP requires the presence of zinc ions in the active site and large structural rotations between closed and open conformational states.

Received: August 7, 2022

Published: December 19, 2022



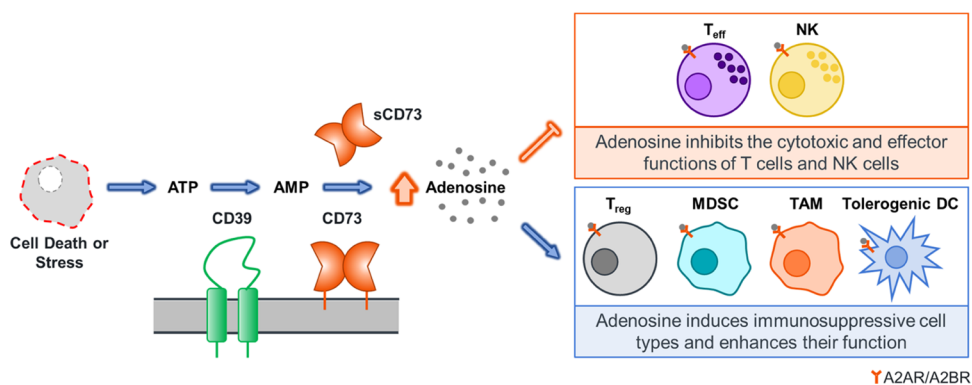


Figure 1. Schematic of the metabolic pathway of adenosine from ATP and its signaling functions in the tumor microenvironment (TME). NK: natural killer; T_{reg}: regulatory T cell; MDSC: myeloid-derived suppressor cell; TAM: tumor-associated macrophage; DC: dendritic cell.

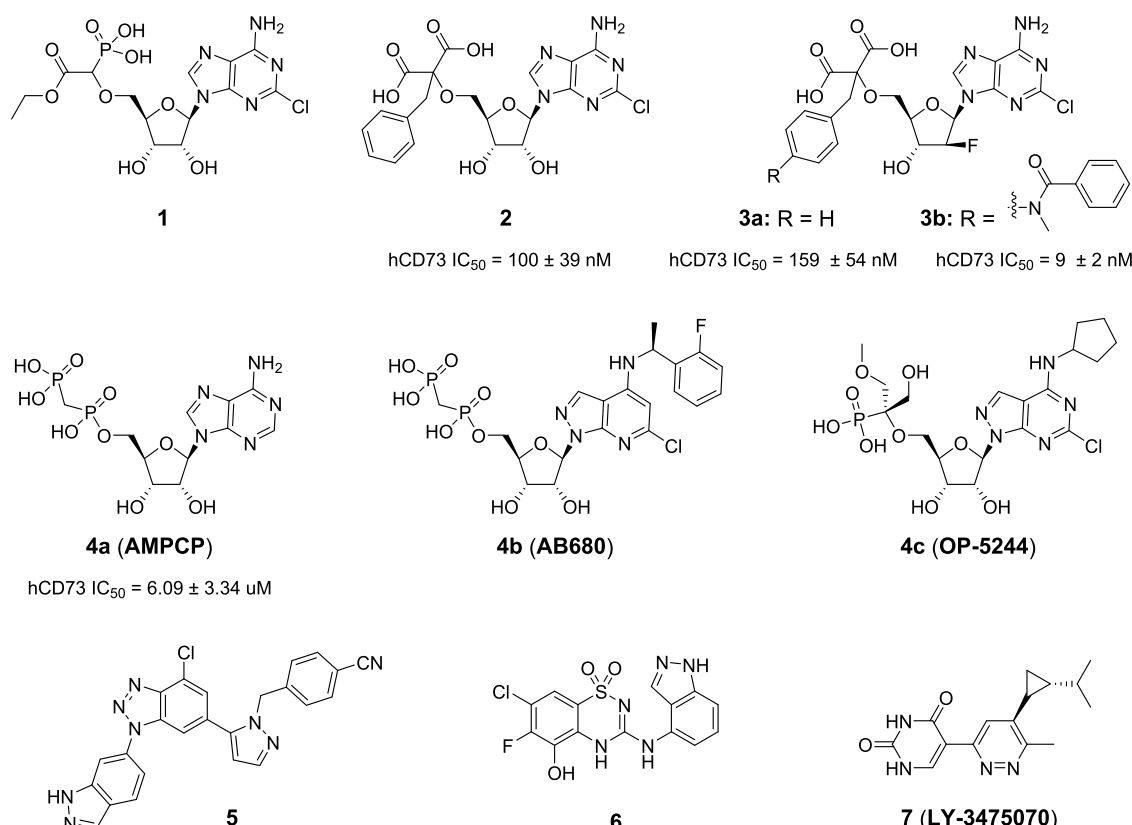


Figure 2. Representative small-molecule CD73 inhibitors. IC₅₀ values of selected compounds against recombinant human CD73 enzyme were determined from in-house assay.

The promising therapeutic potential of targeting CD73 blockade to lower the intratumoral level of ADO has attracted considerable efforts in both preclinical and clinical development of small-molecule and monoclonal antibody CD73 inhibitors.^{27,28} Compared to antibodies, small-molecule inhibitors may have better potential to penetrate into various tissues and through membrane barriers, particularly in solid tumors, and provide a greater exposure within the TME. Several unique classes of small-molecule CD73 inhibitors have been reported in the literature (Figure 2). One class of competitive nucleos(t)ide inhibitors is represented by α -carboxy phosphonate analogues such as (1),²⁹ malonate analogues (2, 3a, and 3b),^{29–31} bis-phosphonate-based analogues (AMPCP (4a)^{32–34} and AB680 (4b)^{35–37}), and mono-phosphonate OP-5244 (4c).³⁸ There are also non-

nucleos(t)ide inhibitors, such as benzotriazole analogue 5;³⁹ benzothiadiazine derivative 6;⁴⁰ and noncompetitive inhibitors exemplified by LY-3475070 (7).⁴¹ It is generally expected that inhibitors with a strong acidic moiety will likely pose challenges during clinical development, particularly due to the potential for poor oral absorption. In addition, some nucleos(t)ide inhibitors exhibited high plasma protein binding that could further limit their effectiveness.⁴²

We have previously disclosed our work on a series of novel and potent 2'- β -fluoro-2'-deoxyribose nucleoside inhibitors against CD73.^{30,31} Although these compounds were able to achieve good potency and on-target *in vivo* efficacy in multiple tumor models, they suffered from several less desirable pharmacokinetic (PK) properties, such as low oral absorption, which was likely due to the high overall polarity and ionic

nature present in their structures. We felt that there was a further need to identify a new class of small-molecule CD73 inhibitors with an improved profile for both potency and physicochemical properties to achieve success in the clinical setting. Herein, we report our discovery and optimization of a novel series of highly potent and selective nucleoside CD73 inhibitors, which culminated in the identification of our orally bioavailable advanced preclinical candidate.

■ RESULTS AND DISCUSSION

Upon the initiation of our discovery efforts, the only publicly available X-ray co-crystal structure of human CD73 was a well-known nucleotide inhibitor, AMPPCP (4a; PDB code: 4H2I). In this crystal structure, the ribose ring adopts a C-3'-endo (North) configuration (Figure 3).²⁶ This active binding

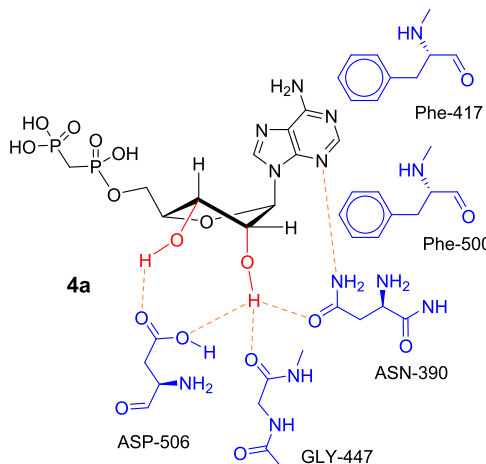


Figure 3. Schematic of conformational analysis of riboside inhibitor AMPPCP (4a, PDB code: 4H2I) binding in the CD73 active site. Amino acids in blue color are protein residues in the CD73 active site.

orientation of the ribose ring is also the preferred configuration for the 2'- α ,3'- α -dihydroxyribose core.^{43,44} Both of these hydroxyl groups on the ribose core of AMPPCP form multiple hydrogen bonding interactions with Asn-390, Gly-447, and Asp-506 in the binding pocket. The purine ring of AMPPCP is sandwiched between Phe-417 and Phe-500 in a double face-to-face π -stacking fashion. In the subsequent years, a similar binding orientation was observed by others for the more potent AMPPCP-based phosphonate analogues.^{32–35,38} However, co-crystallographic structures of the malonic acid class inhibitors, such as 2, have not been described. In our earlier campaign, we designed a series of active 2'- β -fluoro-2'-deoxyribose CD73 inhibitors with the malonic acid moiety, from the early hit 3a ($IC_{50} = 159$ nM) to analogue 3b with improved potency ($IC_{50} = 9$ nM) against recombinant human CD73 enzyme over the reported inhibitor 2.³⁰ However, this new class of 2'- β -fluoro-2'-deoxyribose inhibitors often exhibited some unsatisfactory absorption, distribution, metabolism, and excretion (ADME) properties. Besides the obvious undesirable highly polar and anionic charged characteristic of these nucleoside analogues which often led to inadequate oral exposure, we also observed substantially reduced CD73 inhibitory activity in the presence of full plasma. These issues ultimately prevented the further development of these analogues, and we wanted to focus on addressing these issues in our next generation of CD73 inhibitors. In particular, we felt

that new inhibitors with greater potency could circumvent these hurdles despite the unfavorable physicochemical properties required for the binding interactions with the target.

We turned our attention back to compound 2 and began an exploration of modifying the ribose ring to improve the potency of the malonic acid-based CD73 inhibitors. Initially, a set of analogues with small substitutions (Me, Et, ethynyl, and vinyl) at the C-3'- β -position on the highly steric congested ribose core in compound 2 was prepared. The results of CD73 inhibitory activity for this series of analogues are summarized in Table 1. We were pleased to find that C-3'- β -methyl

Table 1. Structure–Activity Relationships (SAR) of C-3'- β -Substituted Analogue (19, 20, 26, and 27)^{a,b,c}

compound	2	19	20	26	27
R =	H	Me	ethynyl	vinyl	Et
human CD73 ^a IC_{50} (nM)	100 ± 39 ^d	51	1.7 ± 0.22 ^e	103	200
human Cell surface ^b IC_{50} (nM)	434	169	2.8 ± 0.41 ^f		
human plasma CD73 ^c IC_{50} (nM)			5.6 ± 0.24 ^d		
cLog P	−0.37	0.15	0.74	0.39	0.67

^aThe inhibitory activity was evaluated against recombinant human CD73 (0.5 nM) using a malachite green assay. ^bThe inhibitory activity was determined from CD73-expressing SK-MEL-28 cells using a malachite green assay. ^cInhibition of CD73 in plasma was measured using liquid chromatography–mass spectrometry (LC/MS) to assess the conversion of ¹⁵N₅-AMP into ¹⁵N₅-ADO. ^dStandard deviation (SD) value was calculated from two runs. ^eSD value was calculated from four runs. ^fSD value was calculated from three runs.

analogue 19 was able to deliver an improved inhibitory activity against CD73 in both the recombinant human enzyme assay ($IC_{50} = 51$ nM) as the soluble form and CD73-expressing SK-MEL-28 cell surface assay ($IC_{50} = 169$ nM) as the cell surface anchored form. This represented about a 2-fold increase from the parent compound 2 ($IC_{50} = 100$ and 434 nM, respectively).

Our next exploratory target molecule was a 3'- β -ethynyl analogue 20, which presents a linear cylinder-shaped substituent within this congested molecular structure.⁴⁵ To our surprise, this ethynyl analogue 20 was able to provide a remarkable 59 and 145-fold potency improvement over compound 2 when it was evaluated in both the recombinant human enzyme and cell surface CD73 assays ($IC_{50} = 1.7$ and 3 nM, respectively). We also assessed our compounds in the presence of full plasma as a potential indication of their effectiveness in the *in vivo* setting. Fortunately, 20 maintained its inhibitory activity against recombinant human CD73 in the presence of full human plasma by displaying only a modest potency loss ($IC_{50} = 5.6$ nM). Analogue 20 also demonstrated excellent potency ($IC_{50} = 7.3$ nM) against the recombinant mouse CD73 enzyme. The unique cylinder shape of the ethynyl moiety was critical for the remarkable potency increase exhibited by 20. When we evaluated its related alkene 26 and

Table 2. SAR Summary of C-3'- β -Alkyne Analogues (29–30)^{a,b,c}

Compd	R ₁	R ₂	Human CD73 IC ₅₀ ^a (nM)	Human plasma CD73 IC ₅₀ ^b (nM)	Rat iv CL ^c (mL/min/kg)
20	Bn		1.7	5.6	13
29	Bn		1.0	1.6	9.9
30	Bn		0.5	1.5	54

^aThe inhibitory activity was evaluated against recombinant human CD73 (0.05 nM) using a malachite green assay. A lower CD73 enzyme concentration level was applied to accurately assess the inhibitory activity of the more potent new analogues. ^bInhibition of CD73 in plasma was measured using LC/MS to assess the conversion of ¹⁵N₅-AMP into ¹⁵N₅-ADO. ^cRat clearance was determined from iv dosing at a 1 mg/kg dose.

alkane 27 analogues, neither showed any additional benefit over their unsubstituted parent analogue 2.

We next evaluated the pharmacokinetic properties of this highly potent analogue. Although 20 exhibited an improved rat iv clearance (13 mL/min/kg) over 2 (20.4 mL/min/kg), its oral bioavailability remained low (1.8%) from the administration of a dose at 50 mg/kg in the rat oral PK study. This limited oral bioavailability was not unexpected for a highly polar and charged BCS class III molecule such as 20. Despite its low oral exposure, we advanced 20 into mouse *in vivo* studies to assess its antitumor activity via oral administration. We were pleased to find that 20 was able to provide robust *in vivo* efficacy in the EG7 lymphoma mouse xenograft model (data not shown). After observing this initial encouraging result displayed by 20, further SAR work was initiated around this molecule and the results are described in the following section.

Structure–Activity Relationships (SAR). To expand our understanding of the critical role of ethynyl moiety in 20, we sought to further probe its influence by evaluating a set of alkyne analogues (Table 2). We were pleased to find that additional substitution to the ethynyl moiety in 20 provided incremental improvements in CD73 potency. The propyne analogue 29 (IC₅₀ = 1 nM) provided a slight improvement against CD73 enzyme over ethynyl analogue 20 while the more potent cyclopropylethynyl analogue 30 (IC₅₀ = 0.5 nM) was able to deliver a larger 3-fold enhancement. Their CD73 activity (IC₅₀ = 1.6 and 1.5 nM, respectively, for 29 and 30) in full human plasma was also improved with just a slight 1.6 and 3-fold loss from their enzymatic assay. The potency gain exhibited by 30 may be due to an extended π-system created by its sp²-like cyclopropyl group and possible additional hydrophobic interactions with the protein relative to smaller ethynyl analogue 20 and propynyl analogue 29. Unfortunately, the most potent analogue 30 displayed a much higher *in vivo* clearance (54 mL/min/kg) than both 20 and 29 (13 and 9.9 mL/min/kg, respectively) upon iv dosing to rats at a 1 mg/kg dose.

Based on the results from this preliminary SAR work, we propose a plausible binding mode for this series of potent C-3'- β -alkynyl nucleoside CD73 inhibitors (Figure 4). In our

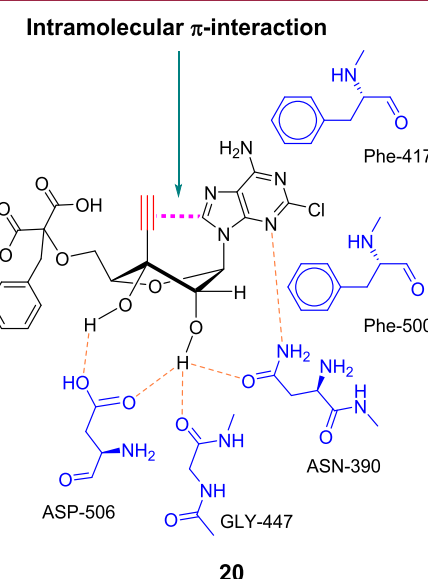
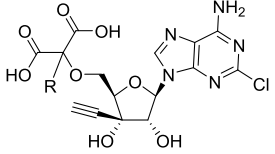


Figure 4. Schematic of a possible stabilization of active C-3'-endo (North) binding conformation through a proposed intramolecular π -interaction. Amino acids in blue color are protein residues in the CD73 active site.

hypothesis, the ribose core with a C-3'- β -alkyne moiety in 20 is expected to maintain the ideal C-3'-endo (North) configuration closely resembling the active binding conformation as seen in AMPCP (Figure 3). The C-3'- β -alkyne moiety in 20 is proposed to make an intramolecular C–H– π interaction between the alkyne and imidazolyl region of the adenine ring. This additional favorable interaction would serve to pre-organize the ligand in the active C-3'-endo ribose core binding conformation, resulting in a lower energy of binding relative to

Table 3. SAR Summary of α -Alkyl Malonic Acid Analogues 34a–j^{a,b}


Compd	R	Human CD73 IC ₅₀ (nM)	Compd	R	Human CD73 IC ₅₀ (nM)
20		1.7 ^a	34e		6 ^a
31	H	58 ^b	34f		5 ^a
34a	Et	24 ^a	34g		9 ^a
34b	Allyl	20 ^a	34h		13 ^a
34c	Propargyl	7 ^b	34i		8 ^a
34d		1.8 ^a	34j		4 ^a

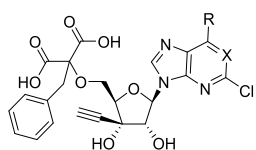
^aThe inhibitory activity was evaluated against recombinant human CD73 (0.05 nM) using a malachite green assay. ^bThe inhibitory activity was evaluated against recombinant human CD73 (0.5 nM) using a malachite green assay. A lower CD73 enzyme concentration level was applied to accurately assess the inhibitory activity of the more potent new analogues.

ligand **2**, which lacks this reinforcement. The 2'- α -3'- α -dihydroxyl group in this C-3'-endo conformation is expected to retain the desirable multiple hydrogen bonding interactions with three key amino acid residues (Asn-390, Gly-447, and Asp-506) in the binding pocket as seen in AMPCP. The requisite combination of both unique features in the new C-3'- β -alkynyl analogue **20** may be responsible for the remarkable increase of inhibitory activity over the previous analogues, which lack the complete set of these structural elements.

We next proceeded to investigate the role of α -benzyl group at the malonate moiety in **20**. The first hint of a contribution to potency by this α -benzyl group was shown by **31**. This analogue, which lacks the α -benzyl group as in **20**, exhibited a substantial 34-fold drop in potency ($IC_{50} = 58$ nM) against recombinant human CD73 enzyme. Therefore, a set of analogues (**34a–j**) with alkyl groups of various sizes ranging from alkyl, alkene, alkyne, and methylaryl was evaluated and the results are reported in **Table 3**. We concluded that factors such as the size, polarity, and electronic characteristics of this α -substitution could influence the CD73 activity. A larger

aromatic ring was generally preferred over a smaller residue. The inhibitory activities for analogues **34a–c** ($R = Et$, allyl, and propargyl) were improved in the increasing order of both their size and π -character although they were still below the potency of **20**. This result suggests that this α -substituent is possibly involved in a π -interaction within its proximity. Heterocyclic analogues (**34e–j**) with a more polar heteroaryl group generally led to a weaker potency ($IC_{50} = 4–13$ nM), except the 3-thiophene analogue **34d** ($IC_{50} = 1.8$ nM) which is about 3-fold more potent than its corresponding 2-thiophene analogue **34e**.

Our next area for exploration of **20** was to modify its adenine ring in an attempt to increase the overall lipophilicity of our targeted molecules. The results from our evaluation of CD73 inhibitory activity for these analogues are summarized in **Table 4**. We first wanted to cap the free NH_2 at the C-6 position of the adenine ring in **20** with various alkyl groups. Except for the *N*-Me analogue **39a** ($IC_{50} = 6$ nM), analogues (**39b–g**) with a hydrophobic mono-*N*-substitution, such as Et, *i*Pr, methylcyclopropane, Bn, and a pair of α -methylbenzyl

Table 4. SAR Summary of Analogs 39a–l and 41 with Adenine Ring Modification^{a,b,c}

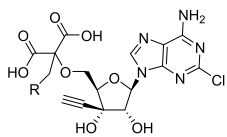
Compd	R	X	cLogP	Human CD73 IC ₅₀ ^a (nM)	Human plasma CD73 IC ₅₀ ^b (nM)	Rat iv CL ^c (mL/min/kg)
20	NH ₂	N	0.74	1.7	5.6	13
39a	NHMe	N	1.57	6	15.5	10
39b	NHEt	N	2.10	1	6.5	7.8
39c		N	2.41	1.7	50	1.4
39d		N	2.54	0.8	11.5	3.7
39e		N	3.02	1	>100	6.3
39f		N	3.32	2	917	1.0
39g		N	3.32	1	208	9.2
39h		N	0.80	2	7.2	7.5
39i		N	1.62	1.1	16	18
39j		N	0.59	0.6	5.4	17
39k		C	3.20	2.0	160	0.91
39l		C	2.48	2.1	41	5.9
41		N	2.66	0.3	136	--

^aThe inhibitory activity was evaluated against recombinant human CD73 (0.05 nM) using a malachite green assay. ^bInhibition of CD73 in plasma was measured using LC/MS to assess the conversion of ¹⁵N₅-AMP into ¹⁵N₅-ADO. ^cRat clearance was determined from iv dosing at a 1 mg/kg dose.

stereoisomers (39f and 39g), generally led to a similar or improved IC₅₀ (ranging from 0.3–1.7 nM) against the recombinant human CD73 enzyme, which suggested various substitutions are tolerated while their overall lipophilicity could be modulated (cLog P = 0.74–3.32). Similar findings for some substitutions were previously explored in the AMPCP-based

bis-phosphonic acid analogues by both Bhattacharai et al.^{32,33} and Lawson et al.³⁵ Finally, both N,N-di-substituted analogues (39i and 39j) also gave a slightly improved potency (IC₅₀ = 1.1 and 0.6 nM, respectively) against the recombinant CD73 enzyme.

A pair of analogues (39k and 39l) with a 3*H*-imidazo[4,5-*b*]pyridine ring showed similar inhibitory activity against the

Table 5. SAR Summary of 4-Substituted Benzyl Analogues (**44a**, **44b**, and **47–49**)^{a,b,c}


R =						
Compound	20	44a	44b	47	48	49
Human CD73 IC ₅₀ ^a (nM)	1.7 ± 0.22 ^d	0.30	0.20	0.10	0.26	0.17 ± 0.02 ^f
Human plasma CD73 IC ₅₀ ^b (nM)	5.6 ± 0.24 ^e	15.6	2.8	0.38	0.26	0.38 ± 0.11 ^f
IC ₅₀ fold shift	3.3	52	14	3.8	1	2.2
Rat iv CL ^c (mL/min/kg)	13	64	2.9			19
cLogP	0.74	2.62	1.57	0.12	1.26	-0.16

^aThe inhibitory activity was evaluated against recombinant human CD73 (0.05 nM) using a malachite green assay. ^bInhibition of CD73 in plasma was measured using LC/MS to assess the conversion of ¹⁵N₅-AMP into ¹⁵N₅-ADO. ^cRat clearance was determined from iv dosing at a 1 mg/kg dose. ^dSD value was calculated from four runs. ^eSD value was calculated from two runs. ^fSD value was calculated from three runs.

recombinant human CD73 enzyme in comparison to their corresponding adenine analogues (**39c** and **39i**), while their cLog P values are increased. Analogue **41** with a thiophene ring in place of the 6-amino group as in **20**, displayed a 5-fold potency enhancement (IC₅₀ = 0.3 nM) against the recombinant human CD73 enzyme. We attribute this potency gain to the possible favorable hydrophobic interaction within the binding pocket produced by the thiophene group. Moreover, the new aryl substitution in **41** also contributes to its enhanced overall lipophilicity from **20** (cLog P = 2.66 vs 0.74).

Maintaining CD73 activity in full plasma was an important parameter in our optimization strategy for the new inhibitors. In particular, having a small shift of CD73 activity in the presence of full plasma would provide better target coverage at a given plasma exposure and may reduce the need for a higher dose regimen *in vivo*. We considered determining the CD73 activity of our compounds in the presence of full plasma would reflect their plasma protein binding profile. The slightly improved CD73 enzyme inhibitory activity of these new *N*-alkyl substitution analogues (**39a–l**) did not lead to a similar improvement in the presence of full human plasma as expected (Table 4). We observed the IC₅₀ values were reduced by 3- to 458-fold in the presence of full human plasma, which was inversely proportional to their lipophilicity trend. The CD73 potency was modestly reduced by about 3- to 4-fold in the presence of plasma for either the unsubstituted parent **20** (IC₅₀ = 1.7 vs 5.6 nM) or the *N*-ethanol analogue **39h** (IC₅₀ = 2 vs 7.2 nM) that has a minimal change in its overall lipophilicity. The more hydrophobic (R)-*α*-methylbenzyl analogue **39f** exhibited an astounding 458-fold reduction of potency in plasma (IC₅₀ = 2 vs 917 nM). Moreover, both 3*H*-imidazo[4,5-*b*]pyridine analogues (**39k** and **39l**) provided an unsatisfactory

loss for their plasma CD73 activity (80- and 20-fold, respectively) which was more than their corresponding more polar adenine analogues (**39c** and **39i**). The most promising hydrophobic analogue **41** delivered a rather disappointing 453-fold potency loss (IC₅₀ = 0.3 vs 136 nM). We reasoned that the observed potency reduction was likely the result of increased plasma protein binding, presumably due to the higher overall lipophilicity of these molecules according to their cLog P values.

To further define the potential benefit of these adenine ring modifications, rat iv PK assessment was performed for selected analogues, and the results are presented in Table 4. All mono-*N*-alkyl analogues (**39a–h**) provided low to moderate rat iv clearance (1.0–10 mL/min/kg), a respectable improvement over **20**. Notably, both the *N*-iPr analogue **39c** and *N*-methylcyclopropyl analogue **39d** exhibited a low clearance (1.4 and 3.7 mL/min/kg, respectively) while maintaining their satisfactory human plasma CD73 activity. In contrast, the *N,N*-di-substituted analogues (**39i** and **39j**) exhibited a higher rat iv clearance (18 and 17 mL/min/kg, respectively) than **20**. The stereo-configuration of *N*-substitution not only influenced the potency but also played a role in the iv clearance rate. Diastereomer **39f** with the (R)-*α*-methylbenzyl residue showed a much lower clearance than its (S)-isomer **39g** (1.0 vs 9.2 mL/min/kg, respectively). It is noteworthy that both the 3*H*-imidazo[4,5-*b*]pyridine analogues (**39k** and **39l**) favorably displayed a lower iv clearance (0.91 and 5.9 mL/min/kg, respectively) than their corresponding adenine analogues (**39c** and **39i**).

While we were pleased to find that the rat iv clearance of our new CD73 inhibitors could be improved by the SAR work described above, the reduction of CD73 activity in the presence of full plasma for some of these analogues raised

concern. Administration of a higher dose would likely be required to maintain the requisite efficacious drug plasma concentration to compensate this potency erosion and could be particularly critical for BCS class III molecules with limited oral bioavailability. Maintaining high CD73 inhibitory activity in the presence of full plasma would allow a lower requirement for oral exposure and circumvent the limited bioavailability issue. We expected to accomplish this goal by either improving the intrinsic activity of our new inhibitors or minimizing their potency attrition in the presence of plasma.

With our goal of increasing the intrinsic potency of the inhibitors, we initiated an exploration of substituents on the benzyl group in **20**, focusing primarily on the para position. The results from this evaluation are summarized in **Table 5**. We were pleased to find that all of these analogues were able to deliver a gain in potency, likely from picking up additional hydrophobic interaction within the binding site. We were initially encouraged by the upgrade of both enzyme potency ($IC_{50} = 0.30$ nM) and lipophilicity ($cLog P = 2.62$) exhibited by the plain biphenyl analogue **44a**, yet we were disappointed to observe both a worsened plasma CD73 activity with a 53-fold reduction and a higher rat iv clearance (64 mL/min/kg) than **20**. However, we were able to reverse both of these trends by incorporating an *ortho*-carboxylic acid moiety on the terminal phenyl ring as in **44b**. Not only did **44b** show both improved plasma CD73 activity and IC_{50} shift, but also it exhibited a rather low rat iv clearance at 2.9 mL/min/kg.

Based on this encouraging result displayed by **44b**, we then proposed to replace the *ortho*-benzoic acid group in **44b** with other polar rings, such as pyridone (**47**), lactam (**48**), and tetrahydropyrimidin-2(1*H*)-one (**49**) that would not bring an additional charge onto the molecules. Gratifyingly, we found all three analogues (**47–49**) with a neutral carbonyl group exhibited either a similar or enhanced enzyme potency in comparison to **44b**. More importantly, they were able to maintain a favorable plasma CD73 activity ($IC_{50} = 0.38$, 0.26, and 0.38 nM, respectively) with little or no IC_{50} shift (1- to 4-fold, respectively) in full human plasma. Compound **49** also showed a moderate rat iv clearance (19 mL/min/kg) similar to **20**. Compound **49** was then chosen for further evaluation based on these favorable findings.

Potency and Selectivity Characterization of 49. In addition to its pico-molar potency against both recombinant human enzyme and plasma CD73 activity, **49** was shown to effectively inhibit the human cell surface CD73 activity ($IC_{50} = 0.21$ nM) from CD73-expressing SK-MEL-28 cells (**Table 6**). Compound **49** was confirmed to be a competitive inhibitor with K_i values of 0.038 and 0.110 nM against the respective human recombinant CD73 and cell surface CD73 enzymes. Compound **49** also displayed favorable activity against mouse recombinant enzyme and plasma CD73 ($IC_{50} = 1.3$ and 1.0 nM, respectively). Treatment of selected cancer patient serum samples (HNSCC, ovarian, TNBC, and esophageal cancers) with **49** confirmed its effective CD73 inhibitory activity ($IC_{50} = 0.10$ –0.21 nM). Compound **49** showed a favorable selectivity for CD73 over its related ecto-enzymes, such as CD39, ectonucleoside triphosphate diphosphohydrolase 2 and 3 (ENTPD2 and ENTPD3) (all $IC_{50} > 10$ μ M) as summarized in **Table 6**.

ADME Profile of 49. Compound **49** displayed a very favorable low to moderate plasma protein binding profile (42–71% bound) across a panel of five species (**Table 7**). In particular, its low human plasma protein binding profile ($f_u =$

Table 6. (A) Summary of CD73 Inhibitory Activity of **49** across Species. **(B)** Selectivity Profile of **49** against Related Ecto-enzymes. **(C)** CD73 Activity of **49** in a Panel of Cancer Patient Serums

(A)	
assay	IC_{50} (nM)
human recombinant CD73 ^{a,c,d}	0.17 ± 0.02^f
human plasma CD73 ^{b,e}	0.38 ± 0.11^f
human cell surface CD73 ^{a,c,d}	0.21 ± 0.12^f
mouse recombinant CD73 ^{a,c,d}	1.3 ± 0.06^g
mouse plasma CD73 ^{b,e}	1.2 ± 0.2^g

cancer patient serum	$CD73 IC_{50}^h$ (nM)
HNSCC	0.21
ovarian cancer	0.15
TNBC	0.18
esophageal	0.10

enzyme	IC_{50} (nM)
CD39 ⁱ	>10,000
ENTPD2 ^j	>10,000
ENTPD3 ^j	>10,000

^{a,c,d}The potency of **49** was evaluated against recombinant CD73 and CD73-expressing SK-MEL-28 cells using a malachite green assay.

^{b,e}Inhibition of CD73 in plasma was measured using LC/MS to assess the conversion of $^{15}\text{N}_5\text{-AMP}$ into $^{15}\text{N}_5\text{-ADO}$. ^fSD value was calculated from three runs. ^gSD value was calculated from two runs. ^hInhibition of CD73 in plasma was measured using LC/MS to assess the conversion of $^{15}\text{N}_5\text{-AMP}$ into $^{15}\text{N}_5\text{-ADO}$. ⁱActivity of cell surface CD39 was assessed using K562 cells expressing human CD39. ^jActivity of recombinant human ENTPD2 and ENTPD3 was assessed.

Table 7. Plasma Protein Binding Profile of **49^a**

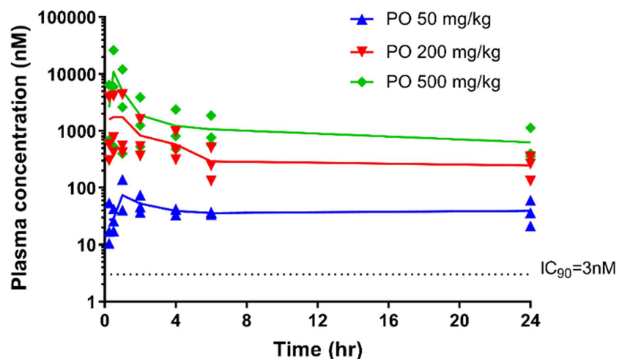
species	mouse	rat	dog	monkey	human
plasma protein binding (% bound)	63%	71%	42%	60%	58%

^aThe data were determined at 10 μ M concentration of **49**.

0.42) is most likely responsible for the minimal loss of its CD73 inhibitory activity in the presence of full plasma, which is highly differentiated from other known CD73 inhibitors.⁴² Moreover, this unique key feature of **49** is expected to provide a sufficient level of unbound drug concentration in systemic exposure despite its expected relatively limited oral bioavailability. A combination of this low protein binding feature and its outstanding pico-molar plasma CD73 activity would likely result in a very favorable pharmacodynamics (PD) effect, which could be achieved with a relatively low systemic exposure requirement in the *in vivo* settings.

Besides the desirable low plasma protein binding, analogue **49** also displayed favorable *in vitro* and *in vivo* properties from the ADME profiling. There was very little observed metabolism when **49** was incubated in the presence of either liver microsomes or hepatocytes from multiple species (mouse, rat, dog, monkey, and human), which was consistent with its polar and charged structural features (**Figure S1**). No CYP450 inhibition was observed against seven major human isoforms (CYP1A2, CYP2B6, CYP2C8, CYP2C9, CYP2C19, CYP2D6, and CYP3A4) at 10 μ M concentration. Although the oral bioavailability of **49** in rats was low ($F = 2.8\%$ at 50 mg/kg

dose), **49** possesses good aqueous solubility (3.88–151 mg/mL) across a broad pH range (1–7), limiting the concern for nonlinear dose relationship *in vivo* due to poor solubility. This was confirmed by the observation of good dose-proportional exposure from oral administration with doses ranging from 50 to 500 mg/kg in the rat PK studies (Figure 5). More



PO Dose (mg/kg)	AUC _{0-24h} (ng*hr/mL)	C _{max} (nM)	T _{max} (hr)
50	580	74	0.8
200	6,094	1,800	0.8
500	18,500	11,000	0.3

Figure 5. Rat oral PK profile of compound **49**. Following PO administration (50 mg/kg) as suspension in 0.5% CMC and 0.1% PS80. The dotted line represents human plasma CD73 IC₉₀ (3 nM).

importantly, plasma drug concentration in these oral PK studies was shown to remain well above the targeted plasma CD73 inhibition (IC₉₀ = 3 nM) for sustained continuous coverage over 24 h.

PK/PD Relationship. Adenosine-mediated suppression of CD8⁺ T cell function (CD25 expression, IFN γ , and granzyme B) and proliferation was reversed by **49** at nanomolar concentrations (Figure S2). Moreover, treatment of **49** at 100 μ M did not exhibit any antiproliferative effects on EG7 (mouse T cell lymphoma) nor A375 (human melanoma) cell lines after 3 days nor on normal human CD8⁺ T cells after 4 days in comparison to the vehicle control (Figure S3).

Besides displaying encouraging good PK exposure in rats, **49** also demonstrated robust PK exposure and pharmacodynamics in mice. Following the administration of a single oral dose at 50 mg/kg to female mice, the plasma exposure of **49** remained above the mouse plasma CD73 IC₅₀ (1.0 nM) for approximately 24 h (Figure 6A). To demonstrate the efficacy and target coverage over time of **49** *in vivo*, EG7 tumor-bearing mice were orally administered 10, 25, and 50 mg/kg doses twice-a-day dosing (BID) for 20 days. Dose-proportional PD response by **49** was demonstrated across doses with a maximal 92% inhibition of plasma CD73 from the highest dose in mice at 2 h post dosing (Figure 6B). Moreover, **49** displayed good penetration into the tumor tissues with a long half-life and was sustained above the human plasma CD73 IC₉₀ (3 nM) after 16 h in the same study and would translate into an extended duration of coverage (Figure 6C).

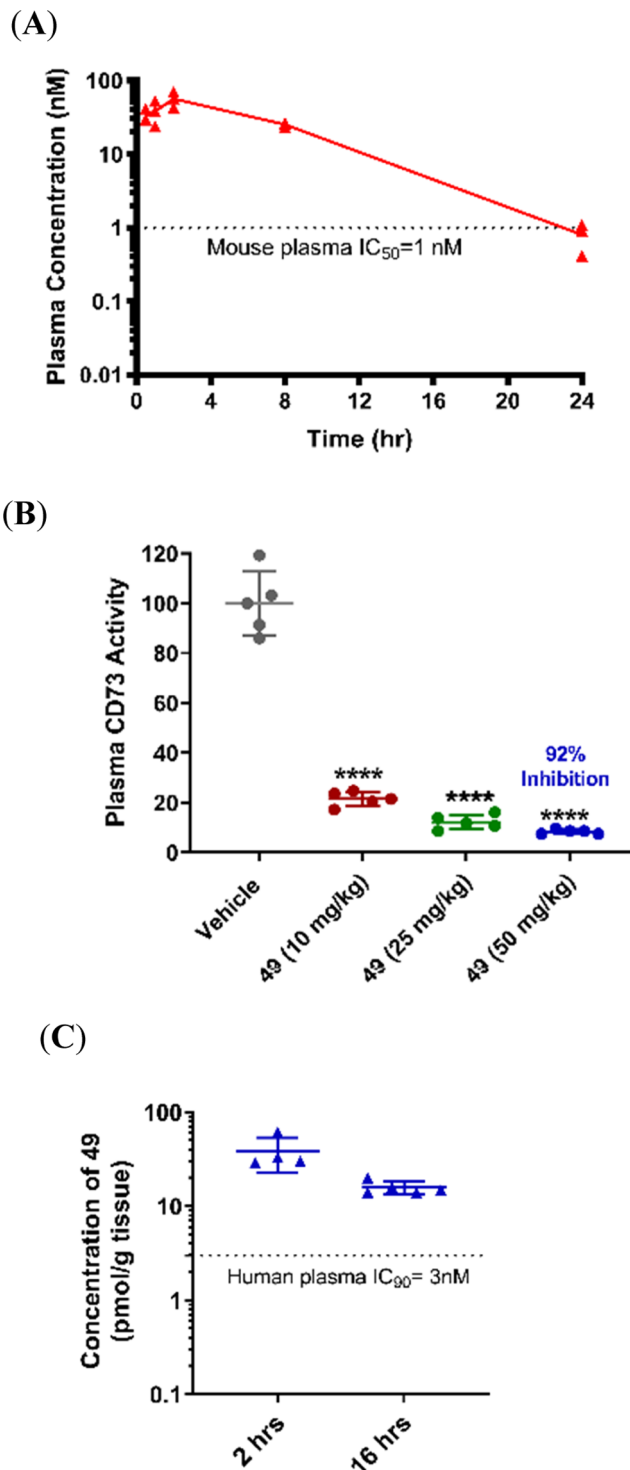


Figure 6. Compound **49** demonstrated sufficient oral exposure and robust pharmacodynamic effect. (A) Single dose **49** (50 mg/kg) was orally administered to female mice and plasma was collected at indicated time points; **49** levels were measured by LC/MS. (B) **49** was orally administered BID to EG7 tumor-bearing mice for 20 days. Plasma was harvested 2 h after the last dose and spiked with ¹⁵N₅-AMP and a TNAP inhibitor. ¹⁵N₅-ADO levels were measured by LC/MS. (C) Tumor tissues from the 50 mg/kg group in (B) were collected 2 or 16 h after the last dose. Levels of **49** were measured by LC/MS. Assumed pmol/g tissue ≈ nM. p-values were generated using one-way ANOVA comparing vehicle-treated animals dosed with **49**. **** ($p < 0.0001$).

In Vivo Efficacy. While several other CD73 small-molecule inhibitors such as **4b** and **4c** demonstrated the PD effect in mice, no single-agent *in vivo* antitumor efficacy has been reported. With the favorable PK/PD result for **49** in hand, we proceeded to evaluate its *in vivo* antitumor efficacy in the mouse xenograft model. We initially assessed its single-agent efficacy with three doses (10, 25, and 50 mg/kg) via oral BID administration in the EG7 mouse lymphoma tumor model and found that robust efficacy was observed for all three chosen doses in a dose-proportional relationship (Figure 7). We were

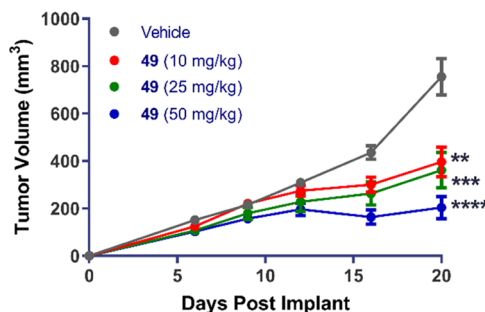


Figure 7. Single-agent antitumor efficacy by **49** in the syngeneic T cell lymphoma EG7 model. (A) EG7 cells were implanted subcutaneously into C57BL/6 mice. **49** (10, 25, and 50 mg/kg) or vehicle was orally administered BID starting on day 1 ($N = 10$ per group) and ending on day 20; p -values were generated using one-way ANOVA comparing end-of-study tumor volumes of compound **49**-treated animals to vehicle-treated animals. **** ($p < 0.0001$); *** ($p < 0.001$); ** ($p < 0.01$).

also able to demonstrate that the antitumor activity shown by **49** in the EG7 model was through the activation of tumor-directed immune response (Figure 8). Compound **49**-treated

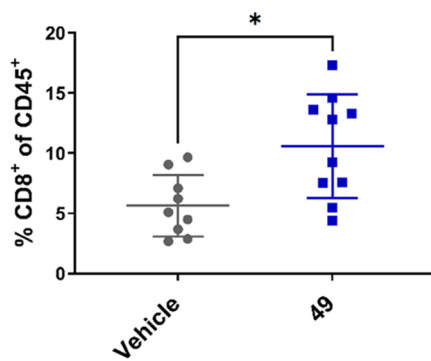


Figure 8. Activation of a tumor-directed immune response by compound **49**. EG7 cells were implanted subcutaneously into C57BL/6 mice. **49** (50 mg/kg) or vehicle was orally administered BID starting day one post implant ($N = 10$ per group). Tumors were excised on day 14 and analyzed by flow cytometry. p -value was generated using Mann–Whitney t -test. * ($p < 0.05$).

mice had increased tumor-infiltrating CD8⁺ cells as determined by flow cytometry following 14-day BID 50 mg/kg dosing. This result supports the conclusion that the antitumor efficacy by **49** in the EG7 model was immune-mediated and there was no tumor intrinsic antiproliferative effect in the *in vitro* cell-based experiments discussed earlier.

We also wanted to investigate the beneficial treatment outcomes for combining **49** with other approved therapeutic agents based on the wealth of preclinical mechanistic work on

CD73 expression and upregulation.^{15,46} Particularly, we focused on both chemo- and immuno-therapeutic treatments that have shown either therapy resistance or high ATP production levels that can lead to elevated immunosuppressive ADO concentration in the TME.^{47,48} It is well known that some chemotherapy agents, such as anthracyclines, platins, and taxanes induce immunogenic cell death (ICD) which results in the release of extracellular ATP.^{49–51} We therefore selected doxorubicin and oxaliplatin as the logical partners for our combination treatments to further enhance their antitumor efficacy. Orally BID administered **49** at 50 or 100 mg/kg dose indeed enhanced the robust antitumor activity in both combination treatments (Figure 9A,B). A robust antitumor efficacy was also demonstrated when **49** was combined with a

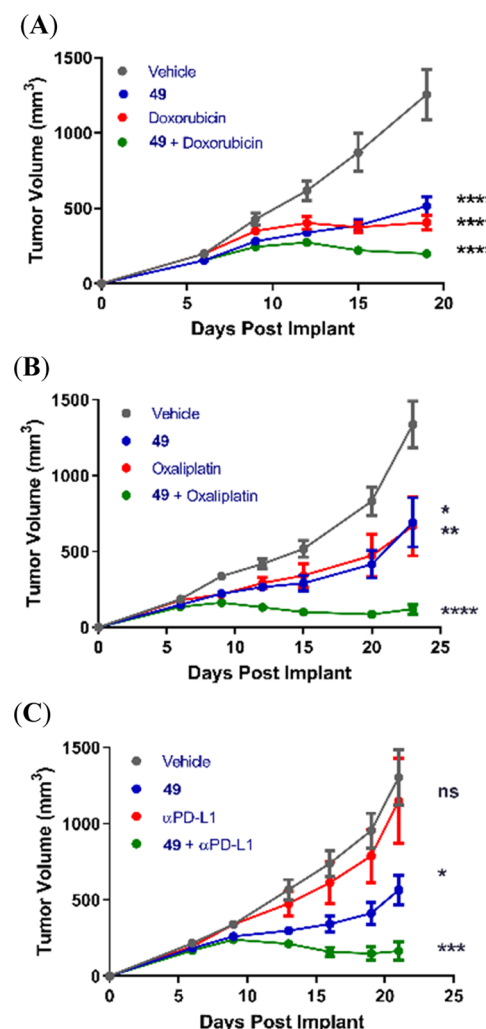
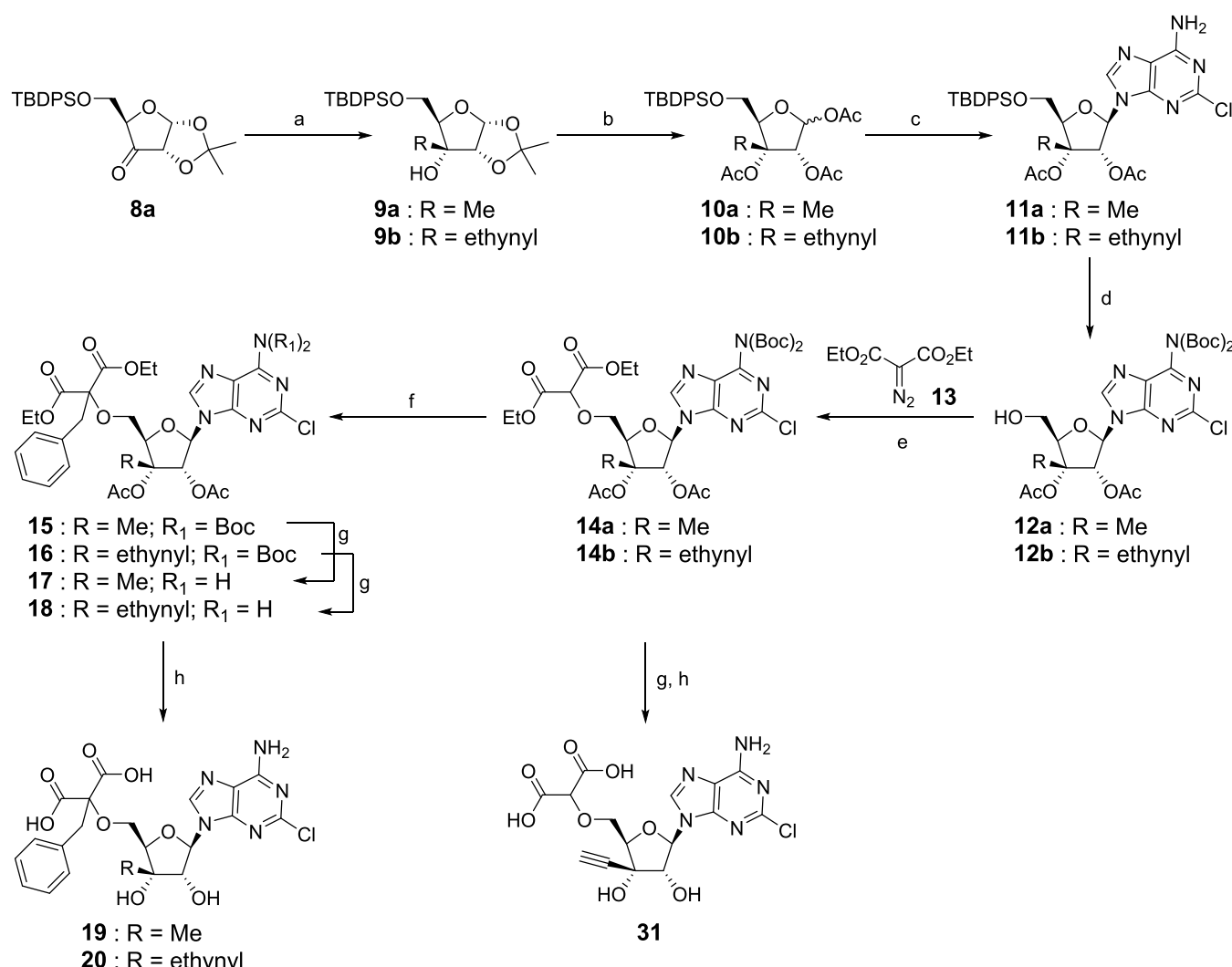


Figure 9. Combination treatments of **49** and chemotherapy agents, oxaliplatin (A), doxorubicin (B), and docetaxel (C). (A–C) EG7 cells were implanted subcutaneously into C57BL/6 mice. (A) **49** (50 mg/kg) or vehicle was orally dosed BID starting on day 1 and ending on day 19. Doxorubicin was dosed iv 2.5 mg/kg. (B) **49** (100 mg/kg) or vehicle was orally dosed BID starting on day 1 and ending on day 23. Oxaliplatin was dosed i.p. 6 mg/kg. (C) **49** (100 mg/kg) or vehicle was orally dosed BID starting on day 1 and ending on day 21. Anti-PD-L1 antibody was dosed i.p. 5 mg/kg. p -values were generated using one-way ANOVA comparing end-of-study tumor volumes of drug-treated animals to vehicle-treated animals. **** ($p < 0.0001$); *** ($p < 0.001$); ** ($p < 0.01$); * ($p < 0.05$); ns (not significant).

Scheme 1. Synthesis of Compounds 19, 20, and 31^a

^aReagents and conditions: (a) MeMgBr or ethynylmagnesium bromide, tetrahydrofuran (THF), 15 °C, 99% for **9a** and 92% for **9b**; (b) (i) aq trifluoroacetic acid (TFA), dichloromethane (DCM), 0–25 °C; (ii) Ac_2O , pyridine, 4-(dimethylamino)pyridine (4-DMAP), DCM, 15 °C, 75% for **10a** and 79% for **10b** over 2 steps; (c) 2-chloroadenine, DBU, TMSOTf, MeCN, 0–65 °C, 57% for **11a** and 54% for **11b**; (d) (i) Boc_2O , triethylamine (TEA), 4-DMAP, *N,N*-dimethylamide (DMF), 20 °C; (ii) tetrabutylammonium fluoride (TBAF), AcOH, THF, 0 °C, 58% for **12a** and 36% for **12b**; (e) $\text{Rh}_2(\text{OAc})_4$, toluene, 25–95 °C, 59% for **14a** and 28% for **14b**; (f) BnBr , K_2CO_3 , DMF, 25 °C, 75% for **15** and 48% for **16**; (g) TFA, DCM, 0–25 °C; (h) LiOH, THF, MeOH or EtOH, H₂O, 25 °C, 65% for **19**, 70% for **20**, 41% for **31** over 2 steps.

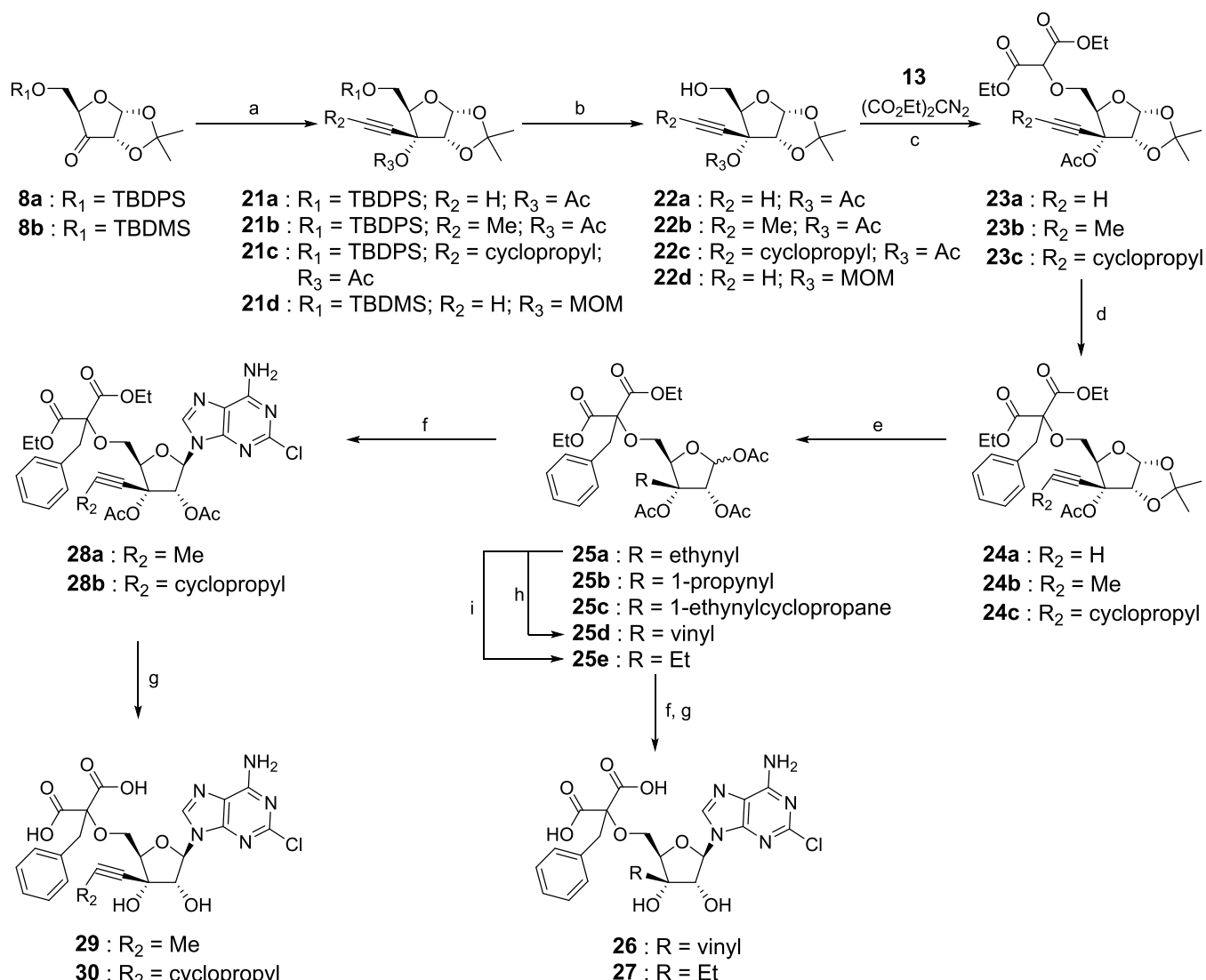
checkpoint inhibitor (Figure 9C). In particular, we were able to observe complete tumor regression in some mice in both the combination treatments with oxaliplatin and anti-PD-L1.

■ CHEMISTRY

The synthesis of 3'-substituted analogues (**19** and **20**) is illustrated in Scheme 1. Treatment of the known ketone precursor **8a**⁵² with MeMgBr gave tertiary alcohol **9a**. The acetonide protecting group in **9a** was removed, and the resulting triol was acetylated to provide the triacetate glycosyl donor **10a** as a mixture of α and β -anomers. Stereoselective glycosylation⁵³ of **10a** with 2-chloroadenine under the influence of 1,8-diazabicyclo[5.4.0]undec-7-ene (DBU) and TMSOTf provided **11a**. The TBDPS group in **11a** was then removed to afford primary alcohol **12a** which then underwent a $\text{Rh}_2(\text{OAc})_4$ -catalyzed carbonyl insertion reaction with ethyl diazomalonate **13** to provide the malonate intermediate **14a**. The benzyl group in **15** was introduced onto the α -position of

diethyl malonate **14a** by alkylation with BnBr . Removal of the Boc groups in **15** led to the penultimate intermediate **17**. Finally, the desired product **19** was obtained cleanly after saponification of all four ester groups in **17**. 3'- β -Ethynyl analogue **20** was synthesized in a similar manner for **19** except substituting MeMgBr with ethynylMgBr. Compound **31** was obtained directly from the deprotection of **14b**.

The preparation of internal alkynyl analogues (**29** and **30**) was accomplished following an alternative approach (Scheme 2). Using the similar chemistry aforementioned, the requisite 3'- β -substitutions (ethynyl, propynyl, and ethynylcyclopropane) were installed onto intermediates **21a–d** which were prepared from either ketone **8a** or **8b**⁵⁴ with the respective ethynylMgBr, propynylMgBr or lithium ethynylcyclopropane reagent *in situ* generated from *n*-BuLi and cyclopropylethyne. The resulting tertiary alcohol intermediates were either acetylated or protected as MOM ether to provide **21a–d**. Removal of the silyl protecting group in **21a–d** provided

Scheme 2. Synthesis of the Corresponding Alkane (26), Alkene (27), and Alkyne (29 and 30) Analogue^a

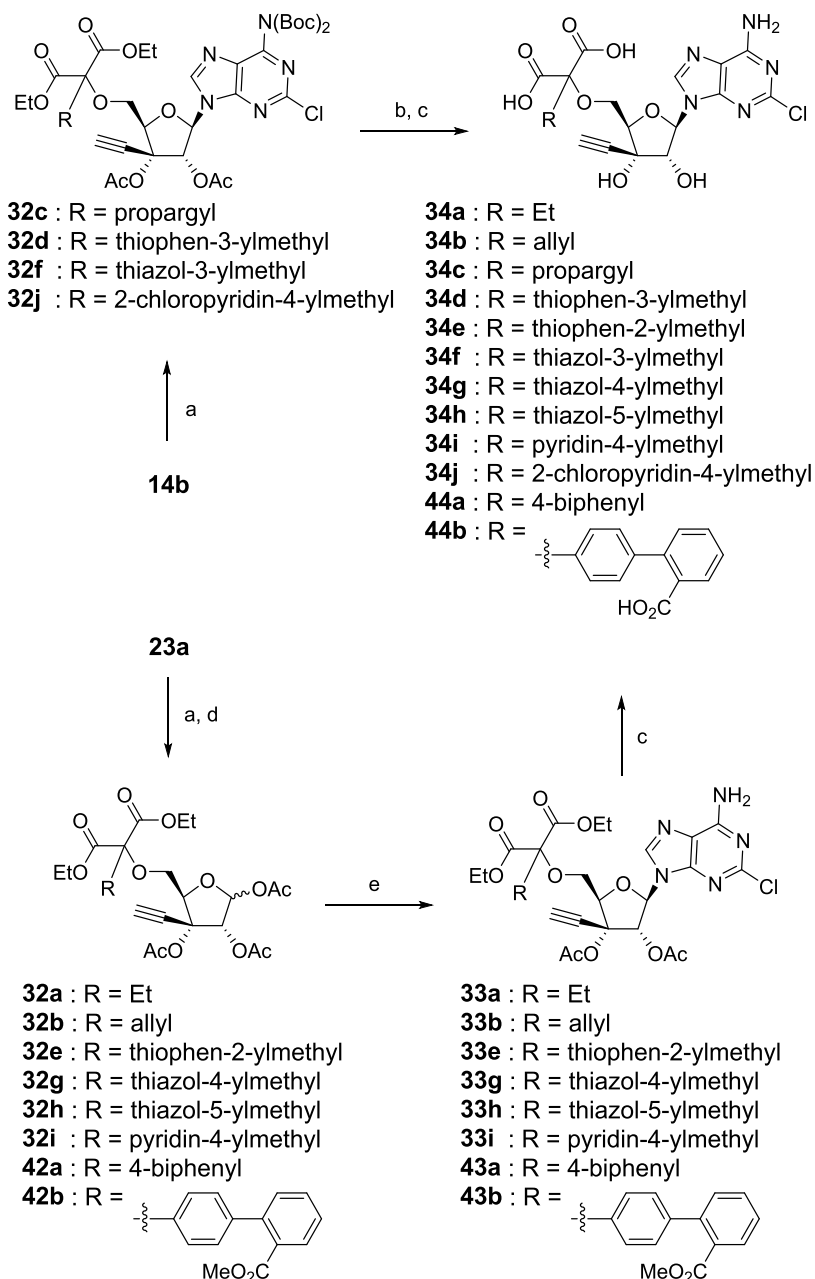
^aReagents and conditions: (a) (i) ethylmagnesium bromide or propynylmagnesium bromide, THF, 20 °C; or (*n*-BuLi and cyclopropylethyne), THF, -78 to 20 °C; (ii) Ac_2O , pyridine, 4-DMAP, DCM, 15 °C; or (iii) NaH, MOMCl, THF, 0–25 °C; (b) TBAF, THF, 0–25 °C, 79% for 22a, 73% for 22b, 74% for 22c, 80% for 22d over 2 steps; (c) diethyl diazomalonate 13, $\text{Rh}_2(\text{OAc})_4$, dichloroethane, 15–40 °C; or toluene, 25–95 °C, 63% for 23a, 80% for 23b, 76% for 23c; (d) BnBr , Cs_2CO_3 or K_2CO_3 , DMF, 20 °C, 92% for 24a, 87% for 24b, 76% for 24c; (e) (i) aq. TFA, DCM, 20 °C; (ii) Ac_2O , pyridine, 4-DMAP, DCM, 20 °C, 78% for 25a, 69% for 25b, 66% for 25c; (f) 2-chloroadenine, DBU or *N,O*-bis(trimethylsilyl)acetamide (BSA), TMSOTf, MeCN, 0–70 °C, 18% for 28a, 23% for 28b; (g) LiOH, THF, H_2O , 25–45 °C, 28% for 26 over 2 steps, 33% for 27 over 2 steps, 23% for 29, 11% for 30; (h) Lindlar catalyst, H_2 , EtOAc , EtOH, 25 °C, 28%; (i) Pd/C , H_2 , EtOAc , 25 °C, 37%.

primary alcohols 22a–d, which were then coupled with diazo reagent 13 via the Rh-catalyzed insertion reaction to give the corresponding malonate products 23a–c. Treatment of 23a–c with BnBr provided acetonide intermediates 24a–c, which were then converted into the respective anomeric triacetate mixture 25a–c via the procedure described above. Stereoselective glycosylation of 25a–c with 2-chloroadenine efficiently provided penultimate intermediates 28a and 28b, which were then saponified to the corresponding di-carboxylic acid products 29 and 30. The related alkene 26 and alkane 27 analogues were synthesized via the selective reductions of alkyne group in intermediate 23a followed by similar glycosylation and deprotection.

The synthesis of a set of analogues (34a–j, 44a, and 44b) with various alkyl groups via two different approaches is illustrated in Scheme 3. In the first approach, the target

molecules (34a–b, 34e, 34g–i, and 44a–b) with the selected alkyl groups at the α -position of malonate moiety were synthesized from precursor 23a and the corresponding halogen electrophiles via the route shown in Scheme 2. Alternatively, the remaining target molecules (34c–d, 34f, and 34j) with other alkyl groups were prepared from precursor 14b and the corresponding halogen electrophiles via intermediates (32c–d, 32f, and 32j) according to the route described in Scheme 1.

A convergent synthesis of a set of *N*-6 substituted analogues (39a–l) was carried out by a regio-selective nucleophilic displacement reaction (Scheme 4). The 2,6-di-chloro intermediate 37 was synthesized from the glycosylation reaction between 2,6-dichloroadenine and intermediate 36, which was prepared from primary alcohol 22d and diazo reagent 35. Regio-selective nucleophilic displacements of the more reactive 6-chloro group in intermediate 37 with various amines

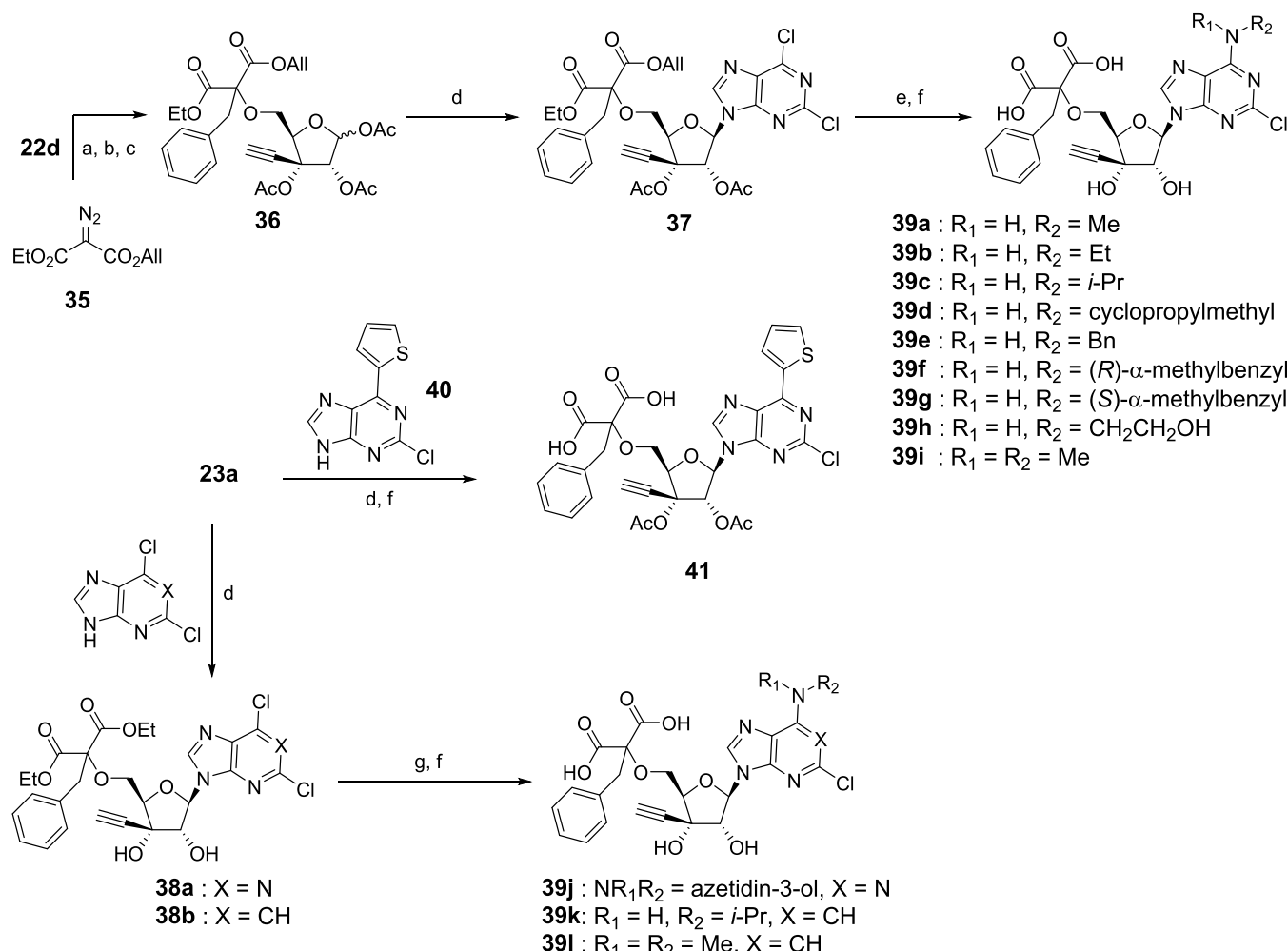
Scheme 3. Synthesis of α -Alkyl Malonic Acid Analogues 34a–j, 44a, and 44b^a

^aReagents and conditions: (a) arylmethyl bromide, Cs₂CO₃ or K₂CO₃, DMF, 20 or 25 °C, 45% for 32c, 68% for 32d, 21% for 32f, and 57% for 32j; (b) TFA, DCM, 0–25 °C; (c) LiOH, THF, H₂O, 25 °C, 36% for 34c over 2 steps, 70% for 34d over 2 steps, 26% for 34f over 2 steps, 86% for 34j over 2 steps, 76% for 34a, 83% for 34b, 53% for 34e, 59% for 34g, 13% for 34h, 3% for 34i, 18% for 44a over 4 steps, and 33% for 44b over 4 steps; (d) (i) aq. TFA, DCM, 0–25 °C; (ii) Ac₂O, pyridine, 4-DMAP, DCM, 20 °C, 78% for 32a, 58% for 32b, 5% for 32e, 31% for 32g, 26% for 32h, and 40% for 32i over 2 steps; (e) 2-chloroadenine, BSA, TMSOTf, MeCN, 0–65 °C, 47% for 33a, 43% for 33b, 34% for 33e, 38% for 33g, 7% for 33h, and 26% for 33i.

followed by the removal of all ester groups in the penultimate intermediates provided the corresponding final products 39a–i. Glycosylation of triacetate precursor 23a with 2,6-dichloroadenine or 5,7-dichloro-3*H*-imidazo[4,5-*b*]pyridine gave the respective key 2,6-dichloro intermediates 38a and 38b. Similarly, a regio-selective nucleophilic displacement reaction between both 38a and 3-hydroxy-azetidine provided the penultimate intermediate, which was followed by the saponification to give 39j. On the other hand, treatment of 38b with *i*-PrNH₂ and TEA in DMF at a higher reaction temperature resulted in the corresponding NH(*i*Pr) and

NMe₂ intermediates which were then converted into a set of products (39k and 39l). Finally, glycosylation reaction of 23a with the corresponding known C⁶-2-thiophenyl-adenine glycosyl acceptor 40 provided the glycoside intermediate that was then converted into the desired final product 41 via the similar process described above.

The set of target molecules (47, 48, and 49) was prepared by the routes according to Scheme 5. First, the synthesis of 47 was achieved through a 4-step sequence. The installation of 4-iodobenzyl group onto precursor 14b by the aforementioned alkylation conditions gave intermediate 45. Coupling of this

Scheme 4. Synthesis of N-Alkyl Analogues 39a–l and 41^a

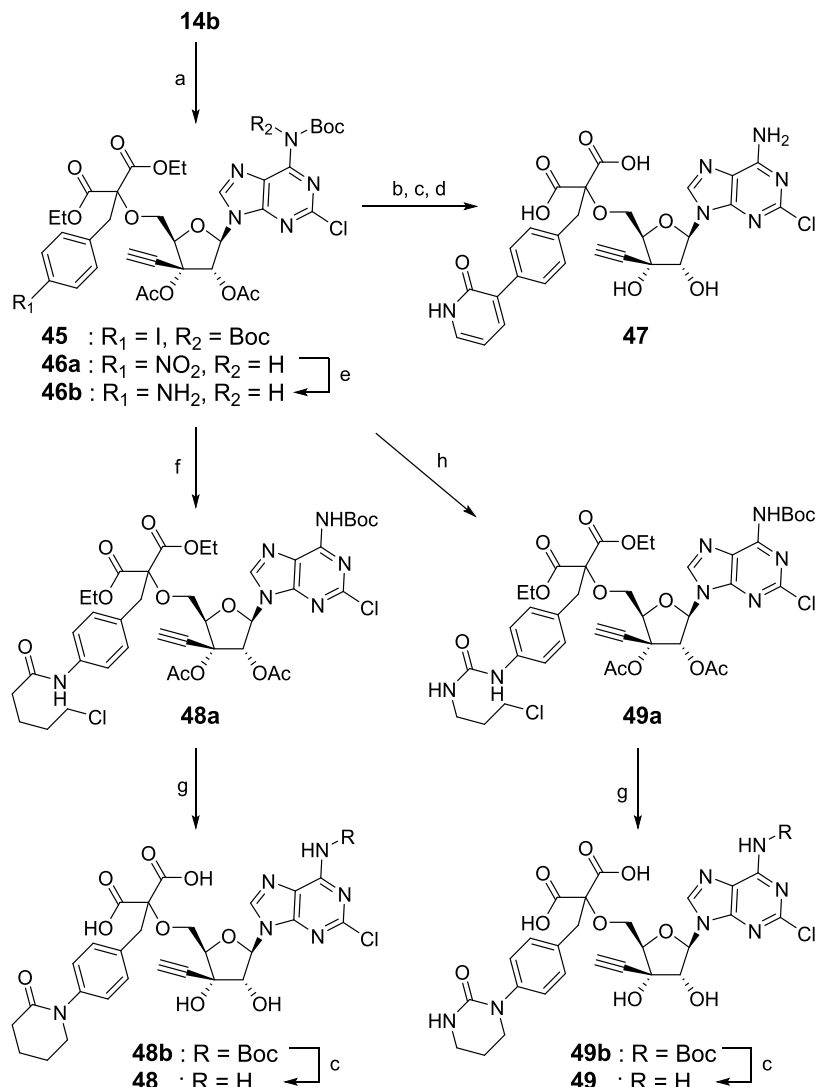
^aReagents and conditions: (a) 1-ethyl 3-(prop-1-en-1-yl) 2-diazomalonate 35, Rh₂(OAc)₄, benzene, 60–65 °C; (b) BnBr, Cs₂CO₃, DMF, 25 °C; (c) AcOH, Ac₂O, Conc. H₂SO₄, 14–17 °C, 58% for 36 over 3 steps; (d) BSA, TMSOTf, MeCN, 25–50 or 25–85 °C, 77% for 37, 29% for 38a, 20% for 38b; (e) HNR₁R₂, dioxane, 0–25 °C; (f) LiOH, THF, H₂O, 25 °C, 77% for 39a, 66% for 39b, 26% for 39c, 37% for 39d, 76% for 39e, 59% for 39f, 52% for 39g, 86% for 39h, 64% for 39i, 48% for 39j, 11% for 39k, 19% for 39l, and 9% for 41 all over 2 steps; (g) i-PrNH₂, or azetidin-3-ol, TEA, DMF, 75 °C.

iodide 45 with (2-oxo-1,2-dihydropyridin-3-yl)boronic acid via a Suzuki reaction provided the corresponding intermediate which was then converted into the final product 47 upon removal of all protecting groups. The synthesis of both compounds 48 and 49 started from introducing the requisite 4-aminobenzyl group onto intermediate 14b via alkylation with 4-nitrobenzyl bromide followed by the reduction of nitro group in 46a to amine 46b. This 4-aminobenzyl intermediate 46b was then converted into either the lactam 48b with 5-chloropentanoyl chloride followed by intramolecular cyclization upon the treatment of the resulting 48a with NaH, or the cyclic urea 49b from 49a with 1-chloropropyl isocyanate under the similar conditions. Finally, removal of the remaining Boc group in both intermediates (48b and 49b) afforded the desired products 48 and 49, respectively.

CONCLUSIONS

In summary, we have discovered a series of novel, highly potent, and orally bioavailable C-3'-β-alkyne nucleoside analogues as CD73 inhibitors based on the reported binding motif of a well-known CD73 inhibitor. The key to this

discovery was the observation of a dramatic increase in potency from the incorporation of a C-3'-β-alkynyl moiety into the ribose core over the known inhibitor 2 with an unmodified natural ribose core. We propose that the unique alkynyl group exerts a favorable intramolecular π-interaction with the adenine ring to preorganize its molecular orientation into the likely active binding conformation. Further optimization on the benzyl tail group in our molecules not only enhanced the intrinsic potency against the CD73 enzyme to the pico-molar level but several analogues also displayed a very minimal loss of CD73 inhibitory activity in the presence of full plasma. Our preclinical work has culminated in the identification of several advanced lead molecules, such as 49, which exhibited a very favorable target coverage over a long duration despite their relatively limited oral bioavailability. These compounds were able to reverse the AMP-mediated suppression of CD8⁺ T cells and completely inhibited the CD73 activity and the ADO production in serum samples from various cancer patients. In the *in vivo* mouse studies, 49 showed robust dose-dependent PK/PD efficacy by reducing the plasma CD73 activity and excellent continuous target coverage over the plasma CD73

Scheme 5. Synthesis of 4-Aryl Analogs 47, 48, and 49^a

^aReagents and conditions: (a) 4-Iodobenzyl bromide or 4-nitrobenzyl bromide, K₂CO₃, DMF, 20–25 °C, 18% for 45, 26% for 46a; (b) (2-oxo-1,2-dihydropyridin-3-yl)boronic acid, Pd(dppf)Cl₂, K₂CO₃, dioxane, H₂O, 20–80 °C; (c) TFA, DCM, 20 °C, 10% for 48, 10% for 49 over 2 steps; (d) LiOH, THF, H₂O, 20 °C, 0.4% for 47 over 3 steps; (e) Fe, NH₄Cl, EtOH, H₂O, 0–50 °C, 13%; (f) 5-chlorovaleryl chloride, TEA, DCM, 0–25 °C, 81%; (g) NaH, THF, 25 °C; (h) 3-chloropropyl isocyanate, TEA, DCM, 0–25 °C, 33%.

IC₅₀. Its mode of action was demonstrated to through the activation of tumor-directed immune response. Altogether, our results suggested that orally administered **49** effectively displayed tumor growth inhibition in mouse xenograft model both as a single agent and in combination with other established chemotherapeutics agents or checkpoint (PD-L1) inhibitor.

These attributes, when coupled with its superb potency profile in the presence of full human plasma and the capability to maintain a relatively large unbound drug level, we believe **49** will have ample exposure in the clinical setting despite its limited oral bioavailability. In addition, **49** gave dose-proportional increases in exposure in rat and was able to achieve multiples of coverage over the target clinical exposure without evidence of PK saturation nor substantial variability. It is anticipated that dose-proportional increases in exposure would also be observed in humans, allowing increased target coverage if needed in the clinic. Altogether, the results from our preclinical work convinced us that **49** would be an effective

CD73 inhibitor to evaluate in the clinic for the treatment of cancers.

EXPERIMENTAL SECTION

General Information. All reagents and solvents were obtained from commercial sources and were used without further purification. Flash chromatographic purification of compounds was performed by utilizing Isco system with pre-packed silica gel cartridges. Compounds purified by preparative reversed-phase high-performance liquid chromatography (HPLC) method were used a Shimadzu system with a Phenomenex Synergi Polar-RP 80A column (4 μm, 150 mm × 20.2 mm) using a gradient mobile phase of H₂O (containing 1% formic acid) and MeCN. Alternatively, the preparative HPLC was performed with a YMC-Triart Pre C18 column (7 μm, 150 mm × 40 mm), or Xtimate C18 column (10 μm, 250 mm × 80 mm) using a gradient mobile phase of water (containing 0.05% NH₃OH + 10 mM NH₄HCO₃, or 0.05–0.225% formic acid) and MeCN. The purity and characterization of compounds were established by a combination of LC-MS and NMR techniques. Final compounds were purified to ≥95% as determined using an LC method on a Shimadzu LC-20AD system with a Phenomenex Luna Phenyl-Hexyl column (100A, 5 μm,

150 mm × 20.2 mm) and UV detection at 230 nm. LC-MS spectra were obtained using an Agilent Technologies 1260 Infinity II liquid chromatography with an Agilent 6120 mass spectrometer (ESI, quadrupole LC-MS) or a Shimadzu LCMS 2010 mass spectrometer (ESI, quadrupole LC-MS). ¹H NMR spectra were recorded on Bruker Instruments operating at 300 and 400 MHz, and using CDCl₃, DMSO-d₆, CD₃OD, or D₂O with data reported as chemical shift in ppm from internal standard tetramethylsilane.

2-(((2R,3S,4R,5R)-5-(6-Amino-2-chloro-9H-purin-9-yl)-3-ethynyl-3,4-dihydroxytetrahydrofuran-2-yl)methoxy)-2-benzylmalonic Acid (20). *Method A.* To a mixture of (3aR,5R,6aS)-5-((tert-butyldiphenylsilyl)oxy)methyl)-2,2-dimethyldihydrofuro[2,3-d][1,3]-dioxol-6(3aH)-one (**8a**) (10 g, 23.44 mmol) in THF (100 mL) at 15 °C under N₂ atmosphere was added a 0.5 M solution of ethynylmagnesium bromide in THF (328 mL, 164 mmol). The mixture was stirred at 15 °C for 16 h before an additional 0.5 M solution of ethynylmagnesium bromide in THF (125 mL) was added and stirred further for 3 h. The mixture was then quenched with saturated aq. NH₄Cl (250 mL) and extracted with EtOAc (3 × 250 mL). The combined organic layer was washed with brine (250 mL), dried over Na₂SO₄, filtered, and concentrated. The crude residue was purified by flash column chromatography on silica gel (0–20% EtOAc in petroleum ether) to provide intermediate **9b** (19.47 g, 92%) as a yellow solid. ¹H NMR (400 MHz, CDCl₃) δ ppm 7.66–7.75 (m, 4H), 7.35–7.47 (m, 6H), 5.85 (d, J = 3.5 Hz, 1H), 4.58 (d, J = 3.8 Hz, 1H), 4.07 (q, J = 5.2 Hz, 1H), 3.97–4.04 (m, 2H), 3.04 (s, 1H), 2.52 (s, 1H), 1.59 (s, 3H), 1.38 (s, 3H), 1.07 (s, 9H); LC/MS (ESI) [M + H]⁺ = 475.0.

To a solution of **9b** (9.47 g, 20.92 mmol) in DCM (100 mL) at 0 °C were added H₂O (10 mL) and TFA (100 mL). The mixture was stirred at 25 °C for 1 h before it was neutralized with saturated aq. NaHCO₃ to pH 7. The aqueous phase was extracted with DCM (2 × 300 mL). The combined organic layer was washed with brine (200 mL), dried over Na₂SO₄, and filtered concentrated. The crude residue was purified by flash column chromatography on a short silica gel plug (0–100% EtOAc in petroleum ether) to provide intermediate (3R,4S,5R)-5-((tert-butyldiphenylsilyl)oxy)methyl)-4-ethynyltetrahydro-furan-2,3,4-triol (5.17 g, 60% yield) as a yellow gum. To a solution of this intermediate (5.17 g, 12.53 mmol) in pyridine (50 mL) at 15 °C was added 4-DMAP (4.59 g, 37.60 mmol) and Ac₂O (11.74 mL, 125.32 mmol). The mixture was stirred at 15 °C for 16 h before H₂O (500 mL) was added and extracted with EtOAc (3 × 200 mL). The combined organic layer was washed with brine (200 mL), dried over Na₂SO₄, filtered, and concentrated. The crude residue was purified by flash column chromatography on silica gel (0–50% EtOAc in petroleum ether) to provide intermediate **10b** as a mixture of α and β-anomers (7.19 g, 79%) and a yellow gum. ¹H NMR (400 MHz, CDCl₃) δ ppm 7.68–7.77 (m, 4H), 7.30–7.46 (m, 6H), 6.50 (d, J = 4.8 Hz, 1H), 5.94 (s, 1H), 5.86 (d, J = 4.8 Hz, 1H), 4.50–4.62 (m, 1H), 4.05 (dd, J = 11.4, 3.4 Hz, 1H), 3.98 (dd, J = 7.5, 4.0 Hz, 1H), 2.66–2.68 (m, 1H), 2.63 (s, 1H), 2.27 (s, 1H), 2.15 (s, 3H), 2.12 (s, 3H), 2.10 (s, 3H), 1.06–1.11 (m, 9H); LC/MS (ESI) [M + H]⁺ = 561.1.

To a solution of **10b** (6.89 g, 12.79 mmol) in MeCN (5 mL) under N₂ atmosphere at 0 °C were added 2-chloroadenine (2.39 g, 14.07 mmol), DBU (5.78 mL, 38.37 mmol), and TMSOTf (11.56 mL, 63.96 mmol). The mixture was stirred at 0 °C for 0.5 h and then at 65 °C for 1 h before it was allowed to cool. The mixture was diluted with saturated aq. NaHCO₃ solution (500 mL) and the aqueous phase was extracted with EtOAc (2 × 350 mL). The combined organic layer was washed with brine (350 mL), dried over Na₂SO₄, filtered, and concentrated. The crude residue was purified by flash column chromatography on silica gel (0–100% EtOAc in petroleum ether) to provide intermediate **11b** (4.52 g, 54%) as a yellow solid. ¹H NMR (400 MHz, DMSO-d₆) δ ppm 8.16 (s, 1H), 7.94 (br s, 12H), 7.61–7.65 (m, 4H), 7.34–7.51 (m, 6H), 6.12–6.19 (m, 2H), 4.63 (t, J = 3.8 Hz, 1H), 4.09 (br d, J = 3.8 Hz, 1H), 4.04 (s, 1H), 2.19 (s, 3H), 2.08 (s, 3H), 1.02 (s, 9H); LC/MS (ESI) [M + H]⁺ = 648.2.

To a solution of **11b** (4.50 g, 6.94 mmol) in DMF (50 mL) at 20 °C were added TEA (4.83 mL, 34.71 mmol), 4-DMAP (254 mg, 2.08

mmol), and Boc₂O (7.58 g, 34.71 mmol). The mixture was stirred at 20 °C for 1 h before H₂O (250 mL) was added, and the resulting mixture was extracted with EtOAc (3 × 230 mL). The combined organic layer was washed with brine (250 mL), dried over Na₂SO₄, filtered, and concentrated. The crude residue was purified by flash column chromatography on silica gel (0–50% EtOAc in petroleum ether) to provide intermediate (2R,3R,4R,5R)-5-(6-(tert-butoxycarbonyl)amino)-2-chloro-9H-purin-9-yl)-2-(((tert-butyldiphenylsilyl)oxy)methyl)-3-ethynyltetrahydrofuran-3,4-diyi diacetate (3.26 g, 55%) as a yellow foam. ¹H NMR (400 MHz, CDCl₃) δ ppm 8.31 (s, 1H), 7.66–7.69 (m, 4H), 7.32–7.46 (m, 6H), 6.29 (d, J = 6.0 Hz, 1H), 6.12 (d, J = 6.0 Hz, 1H), 4.54 (t, J = 3.5 Hz, 1H), 4.16–4.22 (m, 1H), 4.05–4.10 (m, 1H), 4.04 (s, 1H), 2.71 (s, 1H), 2.20 (s, 3H), 2.10 (s, 3H), 1.44 (s, 18H), 1.11 (s, 9H); LC/MS (ESI) [M + H]⁺ = 848.4. To a solution of this intermediate (3.24 g, 3.82 mmol) in THF (35 mL) at 0 °C was added a 1 M solution of TBAF in THF (5.73 mL). The reaction mixture was stirred at 0 °C for 1 h before it was diluted with H₂O (150 mL) and extracted with EtOAc (3 × 130 mL). The combined organic layer was washed with brine (150 mL), dried over Na₂SO₄, filtered, and concentrated. The crude residue was purified by flash column chromatography on silica gel (0–67% EtOAc in petroleum ether) to provide intermediate **12b** (1.51 g, 65%) as a yellow foam. ¹H NMR (400 MHz, CDCl₃) δ ppm 8.40 (s, 1H), 6.23–6.26 (m, 1H), 6.15–6.18 (m, 1H), 4.65 (t, J = 2.4 Hz, 1H), 4.22 (br d, J = 12.3 Hz, 1H), 4.04 (br d, J = 12.7 Hz, 1H), 3.87 (br s, 1H), 2.83 (s, 1H), 2.23 (s, 3H), 2.06 (s, 3H), 1.45 (s, 18H); LC/MS (ESI) [M + H]⁺ = 610.2.

To a solution of **12b** (1.48 g, 2.43 mmol) in toluene (10 mL) under N₂ atmosphere at 20 °C was added Rh₂(OAc)₄ (214 mg, 0.48 mmol) followed by diethyl diazomalonate (**13**) (903 mg, 4.85 mmol) in toluene (3 mL). The mixture was stirred at 95 °C for 2 h before it was cooled to room temperature and concentrated. The crude residue was purified by flash column chromatography on silica gel (0–25% EtOAc in petroleum ether) to provide intermediate **14b** (517 mg, 28%) as a yellow foam. ¹H NMR (400 MHz, CDCl₃) δ ppm 9.02 (s, 1H), 6.33–6.42 (m, 2H), 4.75 (s, 1H), 4.59 (s, 1H), 4.25–4.36 (m, 4H), 4.12–4.18 (m, 1H), 3.99 (dd, J = 10.5, 2.0 Hz, 1H), 2.77 (s, 1H), 2.25 (s, 3H), 2.05 (s, 3H), 1.44 (s, 18H), 1.24–1.33 (m, 6H); LC/MS (ESI) [M + H]⁺ = 768.2.

To a solution of **14b** (497 mg, 0.65 mmol) in DMF (5 mL) at 25 °C was added K₂CO₃ (179 mg, 1.29 mmol). The reaction mixture was stirred for 30 min followed by the addition of benzyl bromide (154 μL, 1.29 mmol). The mixture was stirred at 25 °C for 15.5 h before additional K₂CO₃ (100 mg) and BnBr (100 μL) were added. The mixture was stirred further for 24 h before it was diluted with H₂O (50 mL) and extracted with EtOAc (2 × 50 mL). The combined organic layer was washed with brine (50 mL), dried over Na₂SO₄, filtered, and concentrated. The crude residue was purified by flash column chromatography on silica gel (0–25% EtOAc in petroleum ether) to provide intermediate **16** (266 mg, 48%) as a yellow foam. ¹H NMR (400 MHz, CDCl₃) δ ppm 8.47 (s, 1H), 7.15–7.25 (m, 5H), 6.29 (d, J = 6.5 Hz, 1H), 6.12 (d, J = 6.5 Hz, 1H), 4.66 (t, J = 3.1 Hz, 1H), 4.17–4.26 (m, 4H), 4.12 (d, J = 7.0 Hz, 1H), 4.03 (dd, J = 10.5, 2.8 Hz, 1H), 3.37–3.52 (m, 2H), 2.60 (s, 1H), 2.22 (s, 3H), 2.08 (s, 3H), 1.45 (s, 18H), 1.16–1.27 (m, 6H); LC/MS (ESI) [M + H]⁺ = 858.3.

To a solution of **16** (266 mg, 0.31 mmol) in DCM (3 mL) at 0 °C was added TFA (0.45 mL). The mixture was stirred at 25 °C for 16 h before it was neutralized to pH 7 with saturated aq. NaHCO₃ solution and extracted with DCM (2 × 50 mL). The combined organic layer was washed with brine (50 mL), dried over Na₂SO₄, filtered, and concentrated to provide crude intermediate **18** (195 mg, 96%) as a yellow foam.

To a solution of crude **18** (100 mg, 0.15 mmol) in EtOH (2 mL) at 10 °C was added LiOH·H₂O (18 mg, 0.76 mmol) in H₂O (0.2 mL). The mixture was stirred at 50 °C for 4 h before it was concentrated under reduced pressure. The residue was dissolved in H₂O (15 mL) and extracted with EtOAc (2 × 10 mL). The aqueous phase was separated and acidified to pH 2.5 with 1 N aq. HCl solution and then extracted with EtOAc (3 × 30 mL). The combined organic layer was

washed with brine (10 mL), dried over Na_2SO_4 , filtered, and concentrated to provide the title compound **20** (55 mg, 70%) as a white solid. ^1H NMR (400 MHz, $\text{DMSO}-d_6$) δ ppm 13.00–14.00 (m, 2 H), 8.39 (s, 1 H), 7.79 (br s, 2 H), 7.20 (br d, J = 7.0 Hz, 2 H), 7.01–7.12 (m, 3 H), 5.82 (d, J = 7.5 Hz, 1 H), 4.87 (d, J = 7.8 Hz, 1 H), 4.16 (dd, J = 5.3, 2.5 Hz, 1 H), 3.99–4.07 (m, 2 H), 3.83 (br d, J = 8.0 Hz, 1 H), 3.56 (s, 1 H), 3.25 (dd, J = 6.8 Hz, 2 H); LC/MS (ESI) $[\text{M} + \text{H}]^+$ = 518.0.

2-(((2R,3S,4R,5R)-5-(6-Amino-2-chloro-9H-purin-9-yl)-3,4-dihydroxy-3-(prop-1-yn-1-yl)tetrahydrofuran-2-yl)methoxy)-2-benzylmalonic Acid (29). *Method B.* To a solution of **8a** (10 g, 23.44 mmol) in THF (100 mL) under N_2 atmosphere at 20 °C was added (prop-1-ynyl)magnesium bromide (0.5 M, 93.77 mL). The mixture was stirred at 40 °C for 2 h before it was diluted with saturated aq. NH_4Cl solution (250 mL) and extracted with EtOAc (3 × 200 mL). The combined organic layer was washed with brine (200 mL), dried over Na_2SO_4 , filtered, and concentrated to give crude intermediate (*3aR,5R,6R,6aR*)-*S*-((tert-butylidiphenylsilyl)oxy)methyl)-2,2-dimethyl-6-(prop-1-yn-1-yl)tetrahydrofuro[2,3-*d*][1,3]dioxol-6-ol (11.81 g) as a yellow gum. To a solution of this crude intermediate (12.20 g, 26.14 mmol) in pyridine (120 mL) at 20 °C was added 4-DMAP (3.51 g, 28.76 mmol) and Ac_2O (4.90 mL, 52.29 mmol). The mixture was stirred for 16 h before it was diluted with H_2O (200 mL) and extracted with EtOAc (3 × 100 mL). The combined organic layer was washed with brine (250 mL), dried over Na_2SO_4 , filtered, and concentrated to give the crude intermediate **21b** (15 g) as a yellow gum.

To a solution of crude **21b** (15 g, 29.49 mmol) in THF (300 mL) under N_2 atmosphere at 0 °C was added a 1 M solution of TBAF in THF (44.23 mL, 44.23 mmol) and AcOH (1.26 mL, 22.12 mmol). The mixture was stirred at 20 °C for 7 h before it was diluted with saturated aq. NH_4Cl solution (300 mL) and extracted with EtOAc (3 × 200 mL). The combined organic layer was washed with brine (300 mL), dried over Na_2SO_4 , filtered, and concentrated. The crude residue was purified by flash column chromatography on silica gel (0–50% EtOAc in petroleum ether) to provide intermediate **22b** (5.78 g, 73% over 2 steps) as a white solid. ^1H NMR (400 MHz, CDCl_3) δ ppm 5.87 (d, J = 3.6 Hz, 1H), 5.05 (d, J = 3.7 Hz, 1H), 4.19 (dd, J = 6.9, 4.1 Hz, 1H), 3.88–3.99 (m, 2H), 2.10 (s, 3H), 1.86 (s, 3H), 1.52 (s, 3H), 1.32 (s, 3H).

To a solution of **22b** (5.78 g, 21.39 mmol) in dichloroethane (60 mL) under N_2 atmosphere at 15 °C were added $\text{Rh}_2(\text{OAc})_4$ (945 mg, 2.14 mmol) and diethyl diazomalonate (**13**) (7.96 g, 42.77 mmol). The mixture was stirred at 40 °C for 7 h before it was concentrated. The crude residue was purified by flash column chromatography on silica gel (0–25% EtOAc in petroleum ether) to provide intermediate **23b** (7.30 g, 80%) as a yellow gum. ^1H NMR (400 MHz, CDCl_3) δ ppm 5.84 (d, J = 3.6 Hz, 1H), 5.00 (d, J = 3.7 Hz, 1H), 4.67 (s, 1H), 4.34 (dd, J = 7.7, 2.4 Hz, 1H), 4.23–4.30 (m, 4H), 4.06–4.12 (m, 1H), 3.84 (dd, J = 11.7, 7.7 Hz, 1H), 2.07 (s, 3H), 1.83 (s, 3H), 1.50 (s, 3H), 1.27–1.32 (m, 9H).

To a solution of **23b** (7.28 g, 16.99 mmol) in DMF (70 mL) at 20 °C were added Cs_2CO_3 (11.07 g, 33.98 mmol) and BnBr (3.03 mL, 25.49 mmol). The mixture was stirred for 2 h before it was diluted with H_2O (300 mL) and extracted with EtOAc (3 × 100 mL). The combined organic layer was washed with brine (200 mL), dried over Na_2SO_4 , filtered, and concentrated. The crude product was purified by flash column chromatography on silica gel (0–25% EtOAc in petroleum ether) to provide intermediate **24b** (7.67 g, 87%) as a yellow gum. ^1H NMR (400 MHz, CDCl_3) δ ppm 7.20–7.38 (m, 5H), 5.84 (d, J = 3.6 Hz, 1H), 5.03 (d, J = 3.7 Hz, 1H), 4.31 (dd, J = 7.2, 3.1 Hz, 1H), 4.10–4.18 (m, 4H), 4.04–4.09 (m, 1H), 3.94–4.00 (m, 1H), 3.31–3.41 (m, 2H), 2.08 (s, 3H), 1.82 (s, 3H), 1.52 (s, 3H), 1.33 (s, 3H), 1.19–1.25 (m, 6H).

To a solution of **24b** (7.67 g, 14.79 mmol) in TFA (80 mL) at 20 °C was added H_2O (6.97 mL, 387.05 mmol). The mixture was stirred for 8 h before it was quenched with saturated aq. NaHCO_3 solution to pH 7 and extracted with EtOAc (3 × 100 mL). The combined organic layer was washed with brine (200 mL), dried over Na_2SO_4 , filtered, and concentrated to provide crude intermediate diethyl 2-

benzyl-2-(((2*R*,3*S*,4*R*)-3,4,5-trihydroxy-3-(prop-1-yn-1-yl)-tetrahydrofuran-2-yl)methoxy)malonate (5.95 g) as a yellow gum. To a solution of this crude intermediate (5.95 g, 13.63 mmol) in pyridine (60 mL) at 20 °C was added 4-DMAP (5.00 g, 40.90 mmol) and Ac_2O (6.38 mL, 68.16 mmol). The mixture was stirred for 16 h before it was diluted with H_2O (300 mL) and extracted with EtOAc (3 × 150 mL). The combined organic layer was washed with brine (300 mL), dried over Na_2SO_4 , filtered, and concentrated. The crude product was purified by flash column chromatography on silica gel (0–25% EtOAc in petroleum ether) to provide intermediate **25b** as a mixture of α and β -anomers (5.76 g, 66%, ca. 1:1 ratio) and as a yellow gum. ^1H NMR (400 MHz, CDCl_3) δ ppm 7.20–7.32 (m, 5H), 6.46 (d, J = 4.5 Hz, 0.5H), 6.08 (d, J = 1.0 Hz, 0.5H), 5.71 (d, J = 4.5 Hz, 0.5H), 5.68 (d, J = 1.1 Hz, 0.5H), 4.58 (dd, J = 5.6, 3.2 Hz, 0.5H), 4.49 (dd, J = 6.9, 3.6 Hz, 0.5H), 4.03–4.24 (m, 7H), 3.36 (s, 2H), 2.04–2.11 (m, 9H), 1.84 (m, 3H), 1.20–1.28 (m, 6H); LC/MS (ESI) $[\text{M} + \text{H}]^+$ = 585.1.

To a solution of **25b** (1.00 g, 1.78 mmol) in MeCN (10 mL) under N_2 atmosphere at 20 °C was added *N,N*-bis(trimethylsilyl)acetamide (BSA) (1.32 mL, 5.33 mmol) and 2-chloroadenine (301 mg, 1.78 mmol). The mixture was stirred at 65 °C for 30 min before it was cooled to 0 °C followed by the addition of TMSOTF (642 μL , 3.56 mmol) dropwise. The mixture was stirred at 0 °C for 10 min and then at 65 °C for 2 h before it was quenched with saturated aq. NaHCO_3 (100 mL) and extracted with EtOAc (2 × 60 mL). The combined organic layer was washed with brine (100 mL), dried over Na_2SO_4 , filtered, and concentrated. The crude product was purified by flash column chromatography on silica gel (0–67% EtOAc in petroleum ether) to provide intermediate **28a** (218 mg, 18%) as a foam. ^1H NMR (400 MHz, CDCl_3) δ ppm 8.20 (s, 1H), 7.16–7.20 (m, 5H), 6.19 (d, J = 5.8 Hz, 1H), 5.97 (d, J = 5.8 Hz, 1H), 5.81 (br s, 2H), 4.59–4.64 (m, 1H), 4.14–4.24 (m, 4H), 4.05 (dd, J = 10.5, 3.0 Hz, 2H), 3.35–3.47 (m, 2H), 2.18 (s, 3H), 2.12 (s, 3H), 1.84 (s, 3H), 1.18–1.27 (s, 6H); LC/MS (ESI) $[\text{M} + \text{H}]^+$ = 672.1.

To a solution of **28a** (218 mg, 0.32 mmol) in THF (2 mL) at 20 °C was added LiOH· H_2O (136 mg, 3.24 mmol) in H_2O (2 mL). The mixture was then heated at 45 °C for 2 h before it was allowed to cool, diluted with H_2O (10 mL), and extracted with EtOAc (10 mL). The aqueous phase was separated and acidified to pH 2–3 with 2 N aq. HCl solution before it was extracted with EtOAc (3 × 20 mL). The combined organic layer was washed with brine (30 mL), dried over Na_2SO_4 , filtered, and concentrated. The crude product was purified by preparative reversed-phase HPLC to provide the title compound **29** (39.8 mg, 23%) as a white solid. ^1H NMR (400 MHz, $\text{DMSO}-d_6$) δ ppm 12.70–14.12 (m, 2 H), 8.37 (s, 1H), 7.80 (br s, 2H), 7.19 (br d, J = 7.0 Hz, 2H), 7.00–7.11 (m, 3H), 5.88–6.03 (m, 2H), 5.81 (d, J = 7.5 Hz, 1H), 4.78 (br s, 1H), 4.12 (dd, J = 4.5, 3.0 Hz, 1H), 3.95 (br dd, J = 9.9, 4.9 Hz, 1H), 3.82 (br d, J = 8.5 Hz, 1H), 3.25 (s, 2H), 1.81 (s, 3H); LC/MS (ESI) $[\text{M} + \text{H}]^+$ = 532.0.

2-(((2*R*,3*S*,4*R*,5*R*)-5-(6-Amino-2-chloro-9H-purin-9-yl)-3,4-dihydroxy-3-methyltetrahydrofuran-2-yl)methoxy)-2-benzylmalonic Acid (19). Proceeding as described in Method A for compound **20** above but substituting **9b** with **9a** provided the title compound **19** as a white solid. ^1H NMR (400 MHz, $\text{DMSO}-d_6$) δ ppm 8.38 (s, 1H), 7.77 (br s, 2H), 7.19 (br d, J = 6.5 Hz, 2H), 7.03–7.14 (m, 3H), 5.80 (d, J = 8.0 Hz, 1H), 4.42 (d, J = 8.0 Hz, 1H), 4.00 (m, 1H), 3.60–3.73 (m, 2H), 3.22–3.40 (m, 2H), 1.11 (s, 3H); LC/MS (ESI) $[\text{M} + \text{H}]^+$ = 508.0.

2-(((2*R*,3*S*,4*R*,5*R*)-5-(6-Amino-2-chloro-9H-purin-9-yl)-3,4-dihydroxy-3-vinyltetrahydrofuran-2-yl)methoxy)-2-benzylmalonic Acid (26). A mixture of **25a** (525 mg, 0.96 mmol) and Lindlar catalyst (105 mg, 5 wt %) in EtOH (5 mL) and EtOAc (5 mL) under an atmosphere of H_2 at 25 °C was stirred for 24 h before it was filtered through a pad of diatomaceous earth and rinsed with EtOAc (15 mL). The filtrate was concentrated, and the residue was purified via flash column chromatography on silica gel (0–100% EtOAc in hexanes) to provide intermediate **25d** (25 mg, 28%), which was used directly in the next step without further characterization.

Proceeding as described in Method B for compound **29** above but substituting **25b** with **25d** provided the title compound **26** (28% over

2 steps) as a white solid. ^1H NMR (300 MHz, CD_3OD) δ ppm 8.44 (s, 1H), 7.21–7.22 (m, 2H), 7.06–7.11 (m, 3H), 6.14–6.23 (m, 1H), 6.08–6.10 (d, J = 8 Hz, 1H), 5.55–5.61 (m, 1H), 5.25–5.29 (m, 1H), 4.81 (s, 1H), 4.14 (bs, 1H), 3.91–3.94 (m, 1H), 3.62–3.65 (d, J = 9 Hz, 1H), 3.50–3.55 (d, J = 15 Hz, 1H), 3.39 (s, 1H); LC/MS (ESI) [M + H] $^+$ = 520.1.

2-(((2R,3S,4R,5R)-5-(6-Amino-2-chloro-9H-purin-9-yl)-3-ethyl-3,4-dihydroxytetrahydrofuran-2-yl)methoxy)-2-benzylmalonic Acid (27). A mixture of **25a** (549 mg, 1.0 mmol) and Pd on carbon (100 mg, 10 wt %) in EtOH (5 mL) and EtOAc (5 mL) under an atmosphere of H_2 at 25 °C was stirred for 24 h before it was filtered through a pad of diatomaceous earth and rinsed with EtOAc (15 mL). The filtrate was concentrated, and the residue was purified via flash column chromatography on silica gel (0–100% EtOAc in hexanes) to provide intermediate **25e** (37 mg, 37%), which was used directly in the next step without further characterization.

Proceeding as described in Method B for compound **29** above but substituting **25b** with **25e** provided the title compound **27** (11.5 mg, 33% over 2 steps) as a white solid. ^1H NMR (300 MHz, CD_3OD) δ ppm 8.46 (s, 1H), 7.18–7.20 (m, 2H), 7.04–7.09 (m, 3H), 6.01–6.04 (d, J = 8 Hz, 1H), 4.63–4.66 (d, J = 8 Hz, 1H), 4.21 (bs, 1H), 3.76–3.96 (m, 2H), 3.39–3.52 (m, 2H), 1.76–1.83 (m, 2H), 0.98–1.03 (t, J = 7 Hz, 3H); LC/MS (ESI) [M + H] $^+$ = 522.2.

2-(((2R,3S,4R,5R)-5-(6-Amino-2-chloro-9H-purin-9-yl)-3-(cyclopropylethynyl)-3,4-dihydroxytetrahydrofuran-2-yl)methoxy)-2-benzylmalonic Acid (30). To a solution of ethynylcyclopropane (4.96 g, 75.02 mmol) in THF (80 mL) under a N_2 atmosphere at –78 °C was added a solution of *n*-BuLi in hexanes (2.5 M, 30.01 mL) dropwise. The solution was stirred at –78 °C for 0.5 h followed by the addition of a solution of **8a** (16.0 g, 37.51 mmol) in THF (60 mL) dropwise. The reaction was then allowed to warm to 20 °C and stirred for 1 h before it was cooled to 0 °C and quenched with water (120 mL). The mixture was extracted with EtOAc (2 × 120 mL). The combined organic layer was washed with brine (200 mL), dried over Na_2SO_4 , filtered, and concentrated. The crude residue was purified by flash column chromatography on silica gel (0–15% EtOAc in petroleum ether) to provide intermediate (*3aR,5R,6R,6aR*)-*S*-((*tert*-butyldiphenylsilyl)oxy)methyl)-6-(cyclopropylethynyl)-2,2-dimethyltetrahydrofuro[2,3-*d*][1,3]dioxol-6-ol (15.8 g, 86%) as a syrup. ^1H NMR (400 MHz, CDCl_3) δ ppm 7.68–7.73 (m, 4H), 7.39–7.42 (m, 6H), 5.83 (d, J = 3.5 Hz, 1H), 4.51 (d, J = 3.8 Hz, 1H), 4.04–4.09 (m, 1H), 3.89–4.02 (m, 2H), 2.92 (s, 1H), 1.59 (s, 3H), 1.37 (s, 3H), 1.18–1.25 (m, 1H), 1.08 (s, 9H), 0.73–0.81 (m, 2H), 0.58–0.64 (m, 2H). To a solution of this intermediate (15.8 g, 32.07 mmol) in pyridine (160 mL) at 20 °C was added 4-DMAP (4.70 g, 38.48 mmol) and Ac_2O (9.01 mL, 96.21 mmol). The reaction mixture was stirred for 3 h before it was diluted with water (200 mL) and extracted with EtOAc (2 × 200 mL). The combined organic layer was washed with brine (400 mL), dried over Na_2SO_4 , filtered, and concentrated. The crude residue was purified by flash column chromatography on silica gel (0–15% EtOAc in petroleum ether) to give intermediate **21c** (14.70 g, 86%) as a syrup. ^1H NMR (400 MHz, CDCl_3) δ ppm 7.70–7.73 (m, 4H), 7.36–7.46 (m, 6H), 5.84 (d, J = 3.7 Hz, 1H), 5.02 (d, J = 3.8 Hz, 1H), 4.20–4.25 (m, 1H), 3.94 (dd, J = 5.8, 2.2 Hz, 1H), 2.05 (s, 3H), 1.52 (s, 3H), 1.33 (s, 3H), 1.17–1.18 (m, 1H), 1.08 (s, 9H), 0.67–0.89 (m, 2H), 0.53–0.55 (m, 2H).

Proceeding as described in Method B for compound **29** above but substituting **21b** with **21c** provided the title compound **30** as a white solid. ^1H NMR (400 MHz, CD_3OD) δ ppm 8.04 (s, 1H), 7.14–7.27 (m, 2H), 7.01–7.08 (m, 3H), 5.92 (d, J = 6.6 Hz, 1H), 4.70–4.83 (m, 1H), 4.24 (t, J = 3.5 Hz, 1H), 4.02 (t, J = 3.3 Hz, 2H), 3.31–3.45 (m, 2H), 1.25–1.33 (m, 1H), 0.72–0.79 (m, 2H), 0.63–0.71 (m, 2H); LC/MS (ESI) [M + H] $^+$ = 558.0.

2-(((2R,3S,4R,5R)-5-(6-Amino-2-chloro-9H-purin-9-yl)-3-ethynyl-3,4-dihydroxytetrahydrofuran-2-yl)methoxy)malonic Acid (31). A solution of **14b** (200 mg, 0.26 mmol) in CH_2Cl_2 (1 mL) under an argon atmosphere at 0 °C was added TFA (0.5 mL). The mixture was stirred for 5 min and then at 25 °C for 1 h before additional TFA (0.4 mL) was added. The reaction mixture was stirred for further 1.5 h before it was concentrated. The residue was azeotroped with DCM (5

× 5 mL) to provide crude intermediate diethyl 2-(((2R,3R,4R,5R)-3,4-diacetoxy-5-(6-amino-2-chloro-9H-purin-9-yl)-3-ethynyltetrahydrofuran-2-yl)methoxy)malonate. To a solution of this crude intermediate in a mixture of MeOH (8.5 mL) and water (1.5 mL) at 25 °C was added LiOH· H_2O (86 mg, 2.08 mmol). The resulting mixture was stirred for 16 h before the organic volatile was removed under reduced pressure. The residual aqueous phase was partitioned between water (11 mL) and EtOAc (12 mL). The aqueous phase was separated and acidified to pH 2.5 with 1 N aq. HCl solution before it was extracted with EtOAc (3 × 12 mL). The combined organic layer was dried (Na_2SO_4), filtered, and concentrated to provide the title compound **31** (45.5 mg, 41%) as an off-white solid. ^1H NMR (300 MHz, CD_3OD) δ ppm 8.94 (s, 1H), 6.08 (d, J = 7.5 Hz, 1H), 5.05 (d, J = 7.5 Hz, 1H), 4.65 (s, 1H), 4.29 (t, J = 2.4 Hz, 1H), 4.06 (dd, J = 10.7, 2.5 Hz, 1H), 3.93 (dd, J = 10.6, 2.5 Hz, 1H), 3.12 (s, 1H); LC/MS (ESI) [M + H] $^+$ = 428.0.

2-Allyl-2-(((2R,3S,4R,5R)-5-(6-amino-2-chloro-9H-purin-9-yl)-3-ethynyl-3,4-dihydroxytetrahydrofuran-2-yl)methoxy)malonic Acid (34b). *Method C.* To a solution of **23a** (600 mg, 1.45 mmol) in DMF (1 mL) at 20 °C was added Cs_2CO_3 (943 mg, 2.90 mmol) and allyl bromide (263 mg, 2.17 mmol). The mixture was stirred for 2 h before it was diluted with water (15 mL) and extracted with EtOAc (4 × 10 mL). The combined organic phase was washed with water (10 mL) and brine (10 mL), dried over anhydrous Na_2SO_4 , filtered, and concentrated to provide crude intermediate diethyl 2-(((3*a*R,5*R*,6*R*,6*a*R)-6-acetoxy-6-ethynyl-2,2-dimethyltetrahydrofuro[2,3-*d*][1,3]-dioxol-5-yl)methoxy)-2-allylmalonate (685 mg) as a colorless syrup. To a solution of this crude intermediate (685 mg, 1.51 mmol) in DCM (5 mL) at 20 °C was added TFA (5 mL, 67.53 mmol) and H_2O (1 mL, 55.51 mmol). The mixture was stirred for 16 h before it was diluted with water (15 mL) and adjusted its pH to 7–8 with solid NaHCO_3 . The reaction mixture was extracted with a mixture of DCM and MeOH (4 × 12 mL; 10:1/v:v). The combined extract was washed with saturated aq. NaHCO_3 (8 mL) and brine (8 mL), dried over anhydrous Na_2SO_4 , filtered, and concentrated to give crude intermediate diethyl 2-(((2*R*,3*S*,4*R*)-3-acetoxy-3-ethynyl-4,5-dihydroxytetrahydrofuran-2-yl)methoxy)-2-allylmalonate (580 mg) as a yellowish syrup. To a solution of this crude intermediate (580 mg, 1.40 mmol) in pyridine (5 mL) at 20 °C was added Ac_2O (1.31 mL, 14.00 mmol) and 4-DMAP (513 mg, 4.20 mmol). The mixture was stirred for 15 h before it was diluted with water (15 mL) and extracted with EtOAc (3 × 10 mL). The combined extract was washed with 0.5 N aq. HCl solution (2 × 8 mL), NaHCO_3 (2 × 8 mL) and brine (8 mL), dried over anhydrous Na_2SO_4 , filtered, and concentrated. The crude residue was purified by flash column chromatography on silica gel (17–33% EtOAc in petroleum ether) to give intermediate **32b** as a mixture of α and β -anomers (420 mg, 58%, ca. 1:1 ratio) and as a colorless gum. LC/MS (ESI) [M + H] $^+$ = 521.0.

To a solution of **32b** (360 mg, 0.72 mmol) and 2-chloroadenine (135 mg, 0.79 mmol) in MeCN (5 mL) under N_2 atmosphere at 65 °C was added BSA (446 μL , 1.81 mmol). The mixture was stirred at 65 °C for 0.5 h before it was cooled to 0 °C followed by dropwise addition of TMSOTf (261 μL , 1.44 mmol) in MeCN (1 mL). The reaction mixture was stirred at 65 °C for 3 h before it was allowed to cool, quenched with saturated aq. NaHCO_3 solution (15 mL), and extracted with EtOAc (4 × 10 mL). The combined organic extract was washed with brine (8 mL), dried over anhydrous Na_2SO_4 , filtrated, and concentrated. The crude residue was purified by flash column chromatography on silica gel (20–40% EtOAc in petroleum ether) to give intermediate **33b** (190 mg, 43%) as a white solid. ^1H NMR (400 MHz, CDCl_3) δ ppm 8.67 (s, 1H), 5.86–6.01 (m, 2H), 5.72–5.85 (m, 1H), 5.17 (dd, J = 17.1, 1.4 Hz, 1H), 5.07 (d, J = 10.3 Hz, 1H), 4.72 (t, J = 2.4 Hz, 1H), 4.23–4.35 (m, 4H), 4.09–4.15 (m, 1H), 3.89 (dd, J = 10.3, 1.0 Hz, 1H), 2.87–2.93 (m, 12H), 2.74 (s, 1H), 2.24 (s, 3H), 2.11 (s, 3H), 1.28 (t, J = 7.1 Hz, 3H), 1.18–1.24 (m, 3H); LC/MS (ESI) [M + H] $^+$ = 608.1.

To a solution of **33b** (100 mg, 0.16 mmol) in THF (0.5 mL) and H_2O (0.5 mL) at 25 °C was added LiOH· H_2O (69 mg, 1.64 mmol). The mixture was then stirred at 50 °C for 1 h before it was cooled,

diluted with water (6 mL), and extracted with EtOAc (3×4 mL). The organic phase was discarded. The aq. phase was adjusted to pH 2 with 2 N aq. HCl solution and extracted with EtOAc (4×6 mL). The combined organic phase was washed with brine (6 mL), dried over anhydrous Na₂SO₄, filtered, and concentrated. Lyophilization of this crude residue provided the title compound **34b** (65 mg, 83%) as a white solid. ¹H NMR (400 MHz, CD₃OD) δ ppm 8.83 (s, 1H), 6.05 (d, *J* = 7.5 Hz, 1H), 5.84 (br dd, *J* = 17.2, 10.2 Hz, 1H), 5.15 (dd, *J* = 17.2, 1.6 Hz, 1H), 4.99–5.05 (m, 2H), 4.27 (t, *J* = 2.5 Hz, 1H), 4.00 (dd, *J* = 10.2, 2.6 Hz, 1H), 3.79 (dd, *J* = 10.3, 2.8 Hz, 1H), 3.06 (s, 1H), 2.88 (d, *J* = 7.3 Hz, 2H); LC/MS (ESI) [M + H]⁺ = 467.9.

2-((2R,3S,4R,5R)-5-(6-Amino-2-chloro-9H-purin-9-yl)-3-ethynyl-3,4-dihydroxytetrahydrofuran-2-yl)methoxy)-2-ethylmalonic Acid (34a). Proceeding as described in Method C for compound **34b** above but substituting allyl bromide with EtBr provided the title compound **34a** as a white solid. ¹H NMR (400 MHz, DMSO-*d*₆) δ ppm 8.53–8.83 (m, 1H), 7.81 (br s, 2H), 5.91–6.40 (m, 2H), 5.83 (d, *J* = 7.9 Hz, 1H), 4.91 (d, *J* = 7.7 Hz, 1H), 4.14 (t, *J* = 2.9 Hz, 1H), 3.75 (dd, *J* = 10.3, 3.2 Hz, 1H), 3.56 (s, 1H), 3.47–3.51 (m, 1H), 1.93–2.04 (m, 2H), 0.76 (t, *J* = 7.4 Hz, 3H); LC/MS (ESI) [M + H]⁺ = 455.9.

2-((2R,3S,4R,5R)-5-(6-Amino-2-chloro-9H-purin-9-yl)-3-ethynyl-3,4-dihydroxytetrahydrofuran-2-yl)methoxy)-2-(prop-2-yn-1-yl)-malonic Acid (34c). Proceeding as described in Method A for compound **20** above but substituting BnBr with propargyl bromide provided the title compound **34c** as a white solid. ¹H NMR (300 MHz, CD₃OD) δ ppm 8.96 (s, 1H), 6.07–6.09 (d, *J* = 7.5 Hz, 1H), 5.01–5.04 (d, *J* = 7.5 Hz, 1H), 4.29–4.30 (m, 1H), 3.92–4.05 (m, 2H), 3.01–3.15 (m, 2H), 2.99 (s, 1H), 2.28–2.30 (t, *J* = 2.6 Hz, 1H); LC/MS (ESI) [M + H]⁺ = 465.9.

2-((2R,3S,4R,5R)-5-(6-Amino-2-chloro-9H-purin-9-yl)-3-ethynyl-3,4-dihydroxytetrahydrofuran-2-yl)methoxy)-2-(thiophen-3-ylmethyl)malonic Acid (34d). Proceeding as described in Method A for compound **20** above but substituting BnBr with 3-(bromomethyl)thiophene provided the title compound **34d** as a white solid. ¹H NMR (300 MHz, CD₃OD) δ ppm 8.39 (s, 1H), 7.09–7.17 (m, 2H), 6.98–7.00 (d, *J* = 5.0 Hz, 1H), 6.01–6.04 (d, *J* = 7.5 Hz, 1H), 5.00–5.02 (d, *J* = 7.3 Hz, 1H), 4.32–4.34 (t, *J* = 2.8 Hz, 1H), 4.01–4.11 (m, 2H), 3.41–3.54 (q, *J* = 15.0 Hz, *J* = 9.0 Hz, 2H), 2.98 (s, 1H); LC/MS (ESI) [M + H]⁺ = 524.0.

2-((2R,3S,4R,5R)-5-(6-Amino-2-chloro-9H-purin-9-yl)-3-ethynyl-3,4-dihydroxytetrahydrofuran-2-yl)methoxy)-2-(thiophen-2-ylmethyl)malonic Acid (34e). Proceeding as described in Method C for compound **34b** above but substituting allyl bromide with 2-(bromomethyl)thiophene provided the title compound **34e** as a white solid. ¹H NMR (300 MHz, CD₃OD) δ ppm 8.37 (bs, 1H), 7.10 (d, *J* = 5.0 Hz, 1H), 6.93–6.72 (m, 2H), 6.00 (d, *J* = 7.2 Hz, 1H), 4.98 (d, *J* = 7.6 Hz, 1H), 4.23 (bs, 1H), 4.06 (bs, 2H), 3.62–3.58 (m, 2H), 2.94 (s, 1H); LC/MS (ESI) [M + H]⁺ = 523.9.

2-((2R,3S,4R,5R)-5-(6-Amino-2-chloro-9H-purin-9-yl)-3-ethynyl-3,4-dihydroxytetrahydrofuran-2-yl)methoxy)-2-(thiazol-2-ylmethyl)malonic Acid (34f). Proceeding as described in Method A for compound **20** above but substituting allyl bromide with 2-(bromomethyl)thiazole provided the title compound **34f** as a white solid. ¹H NMR (400 MHz, CD₃OD) δ ppm 8.56 (s, 1H), 7.56 (d, *J* = 3.4 Hz, 1H), 7.33 (d, *J* = 3.4 Hz, 1H), 6.00 (d, *J* = 5.6 Hz, 1H), 4.68–4.73 (m, 1H), 4.38 (dd, *J* = 6.3, 3.4 Hz, 1H), 3.98–4.07 (m, 2H), 3.85 (s, 2H), 3.00 (s, 1H); LC/MS (ESI) [M + H]⁺ = 524.9.

2-((2R,3S,4R,5R)-5-(6-Amino-2-chloro-9H-purin-9-yl)-3-ethynyl-3,4-dihydroxytetrahydrofuran-2-yl)methoxy)-2-(thiazol-4-ylmethyl)malonic Acid (34g). Proceeding as described in Method C for compound **34b** above but substituting allyl bromide with 4-(chloromethyl)thiazole hydrochloride provided the title compound **34g** as a white solid. ¹H NMR (300 MHz, CD₃OD) δ ppm 8.76 (bs, 1H), 8.57 (bs, 1H), 7.36 (bs, 1H), 6.00 (d, *J* = 7.0 Hz, 1H), 5.00–4.95 (m, 1H), 4.35 (bs, 1H), 4.08–4.04 (m, 2H), 3.66–3.64 (m, 2H), 2.98 (s, 1H); LC/MS (ESI) [M + H]⁺ = 524.9.

2-((2R,3S,4R,5R)-5-(6-Amino-2-chloro-9H-purin-9-yl)-3-ethynyl-3,4-dihydroxytetrahydrofuran-2-yl)methoxy)-2-(thiazol-5-ylmethyl)malonic Acid (34h). Proceeding as described in Method C for compound **34b** above but substituting allyl bromide with 5-

(chloromethyl)thiazole provided the title compound **34h** as a white solid. ¹H NMR (400 MHz, CD₃OD) δ ppm 8.75 (s, 1H), 8.47 (s, 1H), 7.72 (s, 1H), 6.03 (d, *J* = 7.3 Hz, 1H), 4.97 (d, *J* = 7.3 Hz, 1H), 4.36 (dd, *J* = 4.3, 3.0 Hz, 1H), 4.12–4.18 (m, 1H), 4.04–4.10 (m, 1H), 3.63–3.79 (m, 2H), 3.00 (s, 1H); LC/MS (ESI) [M + H]⁺ = 524.9.

2-((2R,3S,4R,5R)-5-(6-Amino-2-chloro-9H-purin-9-yl)-3-ethynyl-3,4-dihydroxytetrahydrofuran-2-yl)methoxy)-2-(pyridin-4-ylmethyl)malonic Acid (34i). Proceeding as described in Method C for compound **34b** above but substituting allyl bromide with 4-picolyl chloride hydrochloride provided the title compound **34i** as a white solid. ¹H NMR (300 MHz, CD₃OD) δ ppm 8.50 (bs, 1H), 8.32 (d, *J* = 4 Hz, 2H), 7.50 (d, *J* = 5 Hz, 2H), 6.01 (d, *J* = 7 Hz, 1H), 4.80 (d, *J* = 6 Hz, 1H), 4.38 (q, *J* = 3 Hz, 1H), 4.10–3.95 (m, 2H), 3.45 (bs, 2H), 3.06 (s, 1H); LC/MS (ESI) [M + H]⁺ = 519.0.

2-((2R,3S,4R,5R)-5-(6-Amino-2-chloro-9H-purin-9-yl)-3-ethynyl-3,4-dihydroxytetrahydrofuran-2-yl)methoxy)-2-((2-chloropyridin-4-yl)methyl)malonic Acid (34j). Proceeding as described in Method A for compound **20** above by substituting BnBr with 2-chloro-4-(chloromethyl)pyridine provided the title compound **34j** as a white solid. ¹H NMR (400 MHz, CD₃OD) δ ppm 8.40 (s, 1H), 8.00 (d, *J* = 5.1 Hz, 1H), 7.36 (s, 1H), 7.23 (d, *J* = 5.1 Hz, 1H), 6.01 (d, *J* = 7.6 Hz, 1H), 5.08 (d, *J* = 7.6 Hz, 1H), 4.39 (dd, *J* = 4.9, 2.7 Hz, 1H), 4.16 (dd, *J* = 10.1, 5.2 Hz, 1H), 4.05 (dd, *J* = 10.0, 2.6 Hz, 1H), 3.47 (s, 2H), 3.05 (s, 1H); LC/MS (ESI) [M + H]⁺ = 553.1.

2-([1,1'-Biphenyl]-4-ylmethyl)-2-((2R,3S,4R,5R)-5-(6-amino-2-chloro-9H-purin-9-yl)-3-ethynyl-3,4-dihydroxytetrahydrofuran-2-yl)methoxy)malonic Acid (44a). Proceeding as described in Method C for compound **34b** above but substituting BnBr with 4-biphenyl bromide provided the title compound **44a** as a white solid. ¹H NMR (300 MHz, CD₃OD) δ ppm 8.23 (s, 1H), 7.28–7.43 (m, 9H), 5.99–6.02 (d, *J* = 7.0 Hz, 1H), 4.96–4.98 (d, *J* = 7.0 Hz, 1H), 4.35 (s, 1H), 4.08–4.15 (m, 2H), 3.41–3.57 (m, 2H), 3.04 (s, 1H); LC/MS (ESI) [M + H]⁺ = 594.2.

2-((2R,3S,4R,5R)-5-(6-Amino-2-chloro-9H-purin-9-yl)-3-ethynyl-3,4-dihydroxytetrahydrofuran-2-yl)methoxy)-2-((2'-carboxy-[1,1'-biphenyl]-4-yl)methyl)malonic Acid (44b). Proceeding as described in Method C for compound **34b** above but substituting BnBr with methyl 4'-(bromomethyl)-[1,1'-biphenyl]-2-carboxylate provided the title compound **44b** as a white solid. ¹H NMR (300 MHz, CD₃OD) δ ppm 8.27 (s, 1H), 7.71–7.73 (d, *J* = 7.0 Hz, 1H), 7.29–7.48 (m, 4H), 7.14–7.16 (d, *J* = 8.0 Hz, 1H), 7.08–7.10 (d, *J* = 8.0 Hz, 2H), 5.99–6.01 (d, *J* = 8.0 Hz, 1H), 4.88–4.91 (m, 1H), 4.30 (bs, 1H), 4.03–4.12 (m, 2H), 3.39–3.57 (m, 2H), 2.99 (s, 1H); LC/MS (ESI) [M + H]⁺ = 638.2.

2-Benzyl-2-((2R,3S,4R,5R)-5-(6-Amino-2-chloro-9H-purin-9-yl)-3-ethynyl-3,4-dihydroxytetrahydrofuran-2-yl)methoxy)-malonic Acid (39e). *Method D.* A suspension of NaH (60% in mineral dispersion, 1.91 g, 47.7 mmol) in anhydrous THF (150 mL) at 0 °C was treated with a solution of (3aR,5R,6R,6aR)-5-(((tert-butyldimethylsilyl)oxy)methyl)-6-ethynyl-2,2-dimethyltetrahydrofuro-[2,3-*d*][1,3]dioxol-6-ol (10 g, 30.4 mmol) in THF (50 mL) over 15 min. After stirring for 15 min at 0 °C, the mixture was warmed to room temperature and stirred for an additional 1.5 h. The mixture was then cooled back to 0 °C and treated with MOMCl (6.81 mL, 80.7 mmol) dropwise. The resulting mixture was stirred for 2 h at 25 °C before it was quenched by the slow addition of saturated aq. NH₄Cl (50 mL) and extracted with EtOAc (100 mL). The organic phase was dried over Na₂SO₄, filtered, and concentrated. The crude residue was purified by flash column chromatography on silica gel (30% EtOAc in hexanes) to afford intermediate **21d** (9.95 g, 88%) as a white solid. ¹H NMR (400 MHz, CDCl₃) δ ppm 5.82 (d, *J* = 3.4 Hz, 1H), 5.14 (d, *J* = 6.9 Hz, 1H), 4.76 (d, *J* = 6.9 Hz, 1H), 4.57 (d, *J* = 3.4 Hz, 1H), 4.18 (dd, *J* = 7.0, 3.6 Hz, 1H), 3.99–3.83 (m, 2H), 3.47 (s, 3H), 2.66 (s, 1H), 1.58 (s, 3H), 1.35 (s, 3H), 0.89 (s, 9H), 0.08 (s, 6H).

A solution of **21d** (9.8 g, 26.3 mmol) in anhydrous THF (100 mL) at 0 °C was treated with 1 M solution of TBAF in THF (37 mL, 36.8 mmol). The reaction was warmed to 25 °C and stirred for 3 h before it was concentrated. The viscous residual oil was purified by flash column chromatography on silica gel (0–50% EtOAc in hexanes) to give intermediate **22d** (6.18 g, 91%) as a white solid. ¹H NMR (400

MHz, CDCl₃) δ ppm 5.83 (d, *J* = 3.4 Hz, 1H), 5.11 (d, *J* = 6.9 Hz, 1H), 4.82 (d, *J* = 6.9 Hz, 1H), 4.62 (d, *J* = 3.4 Hz, 1H) 4.24 (t, *J* = 5.5 Hz, 1H), 3.94 (d, *J* = 5.5 Hz, 2H) 3.47 (s, 3H) 2.73 (s, 1H), 1.59 (s, 3H), 1.36 (s, 3H).

A solution of malonic acid monoethyl ester (10.6 g, 80.2 mmol) and 4-DMAP (0.25 g, 2 mmol) in allyl alcohol (11 mL, 160.5 mmol) was added dropwise to a solution of dicyclohexylcarbodiimide (DCC, 18.54 g, 89.9 mmol) in DCM (80 mL) at 0 °C. After stirring for 12 h, the mixture was filtered over Celite and washed with additional DCM. The filtrate was concentrated *in vacuo*, dissolved in EtOAc (50 mL), washed with water (2 × 50 mL), dried over sodium sulfate, and concentrated to afford 1-ethyl 3-prop-2-en-1-yl propandioate (13.4 g, 97%) as a light-yellow oil. To a mixture of 1-ethyl 3-prop-2-en-1-yl propandioate (11.72 g, 68.07 mmol) and 4-acetamidobenzene-1-sulfonyl azide (16.35 g, 68.07 mmol) in MeCN (35 mL) at 0 °C was added Et₃N (18.92 mL, 136.1 mmol). The mixture was stirred at 0 °C for 2 h and then at room temperature overnight. The precipitate was removed by filtration. The filtrate was concentrated *in vacuo* and purified by silica gel column chromatography (20% EtOAc in hexanes) to afford intermediate 35 (12.8 g, 95%) as a colorless oil. ¹H NMR (400 MHz, CDCl₃) δ ppm 5.94 (ddt, *J* = 17.2, 10.4, 5.7 Hz, 1H), 5.36 (dt, *J* = 17.2, 1.5 Hz, 1H), 5.27 (dq, *J* = 10.4, 1.3 Hz, 1H) 4.73 (dt, *J* = 5.7, 1.4 Hz, 2H), 4.30 (q, *J* = 7.1 Hz, 2H), 1.32 (t, *J* = 7.1 Hz, 3H). LC/MS (ESI) [M + H]⁺ = 199.0.

A solution of alcohol 22d (175 mg, 0.68 mmol) and 1-ethyl 3-(prop-1-en-1-yl) 2-diazomalonate (35) (188 mg, 0.95 mmol) in anhydrous benzene (8 mL) was treated with Rh₂(OAc)₄ (5.80 mg, 0.013 mmol) and warmed to 60–65 °C for 2 h. The reaction mixture was concentrated and the crude residue was purified by flash column chromatography on silica gel (0–50% EtOAc in hexanes) to afford intermediate 1-ethyl 3-((E)-prop-1-en-1-yl) 2-(((3aR,5R,6R,6aR)-6-ethynyl-6-(methoxymethoxy)-2,2-dimethyltetrahydrofuro[2,3-d][1,3]dioxol-5-yl)methoxy)malonate as a mixture of diastereomers (*ca.* 1:1 ratio, 252 mg, 87%) and as a pale yellow oil. A solution of this intermediate (250 mg, 0.58 mmol) and BnBr (0.42 mL, 3.50 mmol) in anhydrous DMF (8 mL) under N₂ atmosphere was treated with Cs₂CO₃ (760 mg, 2.33 mmol) and stirred at 25 °C for 4 h before it was filtered through a pad of Celite. The filtrate was diluted with water and extracted with EtOAc. The organic layer was dried over Na₂SO₄, filtered, and concentrated. The crude residue was purified by flash column chromatography on silica gel (30% EtOAc in hexanes) to afford intermediate 1-ethyl 3-prop-1-en-1-yl 2-benzyl-2-(((3aR,5R,6R,6aR)-6-ethynyl-6-(methoxymethoxy)-2,2-dimethyltetrahydrofuro[2,3-d][1,3]dioxol-5-yl)methoxy)malonate as a mixture of diastereomers (*ca.* 1:1 ratio, 261 mg, 86%) as a pale yellow oil. A solution of this intermediate (500 mg, 0.96 mmol) in AcOH (3.9 mL) at 14–17 °C was treated with Ac₂O (0.96 mL, 10.3 mmol) and concentrated sulfuric acid (410 μL, 0.33 mmol). The resulting mixture was stirred for 4 h before it was diluted with water and extracted with EtOAc. The organic layer was washed with saturated aq. NaHCO₃ (100 mL), dried (Na₂SO₄), filtered, and concentrated. The residual oil was purified by flash column chromatography on silica gel (0–50% EtOAc in hexanes) to provide intermediate 36 as a mixture of α and β-anomers (420 mg, 78%) and as a clear oil. ¹H NMR of the major product (400 MHz, CDCl₃) δ ppm 7.27–7.20 (m, 5H), 6.44 (d, *J* = 4.7 Hz, 1H), 5.89–5.82 (m, 1H) 5.75 (d, *J* = 4.7 Hz, 1H), 5.30 (ddd, *J* = 17.2, 3.3, 1.6 Hz, 1H), 5.24–5.21 (m, 1H), 4.63–4.59 (m, 3H), 4.22–4.16 (m, 2H), 4.10–4.06 (m, 2H), 3.37–3.35 (m, 2H), 2.61 (s, 1H), 2.11 (s, 6H), 2.07 (s, 3H), 1.22 (t, 3H, *J* = 7.1 Hz). LC/MS (ESI) [M + Na]⁺ = 583.0.

A suspension of 2,6-dichloroadenine (143 mg, 0.76 mmol) and N,O-bis(trimethylsilyl)acetamide (0.24 mL, 0.97 mmol) in anhydrous MeCN (5 mL) 25 °C was treated with a solution of 36 (420 mg, 0.75 mmol) in anhydrous MeCN (15 mL) followed by dropwise addition of TMSOTf (0.18 mL, 1.00 mmol). The reaction was warmed to 50 °C for 18 h and then cooled to room temperature. The reaction was quenched with saturated aq. NaHCO₃ solution, and the mixture was stirred for 10 min before it was extracted with EtOAc (3 × 30 mL). The combined organic layer was dried over Na₂SO₄, filtered, and concentrated. The crude residue was purified by flash column

chromatography on silica gel (0–50% EtOAc in hexanes) to give intermediate 37 as a mixture of diastereomers (400 mg, 77%, *ca.* 1:1 ratio) and as a white solid. ¹H NMR (400 MHz, CDCl₃) δ ppm 8.56 (d, *J* = 12.1 Hz, 1H), 7.22–7.19 (m, 2H), 7.14–7.11 (m, 3H), 6.26 (d, *J* = 6.6 Hz, 1H), 6.14 (d, *J* = 6.6 Hz, 1H), 5.89–5.75 (m, 1H), 5.34–5.18 (m, 2H), 4.67–4.57 (m, 3H), 4.24 (p, *J* = 7.1 Hz, 2H), 4.17–4.04 (m, 2H), 3.50 (d, *J* = 14.7 Hz, 1H), 3.40 (d, *J* = 14.7 Hz, 1H), 2.62 (d, *J* = 5.4 Hz, 1H), 2.23 (s, 3H), 2.21 (s, 3H), 1.22 (t, *J* = 7.1 Hz, 3H). LC/MS (ESI) [M + Na]⁺ = 711.1.

A solution of 37 (80 mg, 0.12 mmol) in anhydrous dioxane (2 mL) at 0 °C was treated with DIPEA (30 μL, 0.17 mmol) and benzylamine (13 μL, 0.12 mmol). The reaction was warmed to room temperature and stirred for 18 h before it was diluted with water (20 mL) and extracted with EtOAc (50 mL). The organic layer was dried over Na₂SO₄, filtered, and concentrated. The crude product was purified by flash column chromatography on silica gel (50% EtOAc in hexanes) to provide intermediate 1-ethyl 3-prop-1-en-1-yl 2-benzyl-2-(((2R,3R,4R,5R)-3,4-diacetoxy-5-(6-(benzylamino)-2-chloro-9H-purin-9-yl)-3-ethynyltetrahydrofuran-2-yl)methoxy)malonate as a mixture of diastereomers (*ca.* 1:1 ratio, 75 mg, 85%). A solution of this intermediate (70 mg, 0.092 mmol) in THF (1 mL) and H₂O (1 mL) at 25 °C was treated with LiOH·H₂O (31 mg, 1.35 mmol) and stirred for 18 h. The reaction was acidified with 2 N aq. HCl solution to pH 3. The resulting suspension was stirred for 10 min before the precipitate was collected by filtration, washed with cold water, and dried to provide the title compound 39e (50 mg, 89%) as a white solid. ¹H NMR (400 MHz, CDCl₃/CD₃OD = 5:1/v:v) δ ppm 7.98 (s, 1H), 7.25–6.84 (m, 10H), 5.85 (d, *J* = 6.4 Hz, 1H), 4.63 (s, 2H), 4.54 (d, *J* = 6.4 Hz, 1H), 4.17 (t, *J* = 3.2 Hz, 1H), 3.88 (qd, *J* = 10.3, 3.3 Hz, 2H), 3.36–3.16 (m, 2H), 2.49 (s, 1H); LC/MS (ESI) [M + H]⁺ = 608.1.

2-Benzyl-2-(((2R,3S,4R,5R)-5-(2-chloro-6-(methylamino)-9H-purin-9-yl)-3-ethynyl-3,4-dihydroxytetrahydrofuran-2-yl)methoxy)malonic Acid (39a). Proceeding as described in Method D for compound 39e above but substituting benzylamine with methylamine provided the title compound 39a as a white solid. ¹H NMR (400 MHz, CD₃OD) δ ppm 8.18 (s, 1H), 7.29–7.20 (m, 2H), 7.04 (dd, *J* = 5.1, 1.9 Hz, 3H), 5.99 (d, *J* = 7.4 Hz, 1H), 4.99 (d, *J* = 7 Hz, 1H), 4.30 (t, *J* = 3.3 Hz, 1H), 4.11–4.01 (m, 2H), 3.49–3.34 (m, 2H), 3.06 (s, 3H), 2.98 (s, 1H); LC/MS (ESI) [M + H]⁺ = 532.1.

2-Benzyl-2-(((2R,3S,4R,5R)-5-(2-chloro-6-(ethylamino)-9H-purin-9-yl)-3-ethynyl-3,4-dihydroxytetrahydrofuran-2-yl)methoxy)malonic Acid (39b). Proceeding as described in Method D for compound 39e above but substituting benzylamine with ethylamine provided the title compound 39b as a white solid. ¹H NMR (400 MHz, CD₃OD) δ ppm 8.16 (s, 1H), 7.40–7.19 (m, 2H), 7.04 (dd, *J* = 5.1, 1.9 Hz, 3H), 5.98 (d, *J* = 7.4 Hz, 1H), 4.97 (d, *J* = 7.4 Hz, 1H), 4.30 (t, *J* = 3.3 Hz, 1H), 4.14–3.98 (m, 2H), 3.57 (d, *J* = 7.8 Hz, 2H), 3.49–3.33 (m, 2H), 2.98 (s, 1H), 1.28 (t, *J* = 7.2 Hz, 3H); LC/MS (ESI) [M + H]⁺ = 546.1.

2-Benzyl-2-(((2R,3S,4R,5R)-5-(2-chloro-6-(isopropylamino)-9H-purin-9-yl)-3-ethynyl-3,4-dihydroxytetrahydrofuran-2-yl)methoxy)malonic Acid (39c). Proceeding as described in Method D for compound 39e above but substituting benzylamine with isopropylamine provided the title compound 39c as a white solid. ¹H NMR (400 MHz, CD₃OD) δ ppm 8.05 (s, 1H), 7.23–7.12 (m, 2H), 7.09–6.78 (m, 3H), 5.91 (d, *J* = 6.2 Hz, 1H), 4.59 (d, *J* = 6.2 Hz, 1H), 4.37 (m, 1H), 4.28 (m, 1H), 3.42 (d, *J* = 14.8 Hz, 1H), 3.35–3.22 (m, 3H), 2.56 (s, 1H), 1.24 (d, *J* = 6.5 Hz, 6H); LC/MS (ESI) [M + H]⁺ = 560.0.

2-Benzyl-2-(((2R,3S,4R,5R)-5-(2-chloro-6-((cyclopropylmethyl)amino)-9H-purin-9-yl)-3-ethynyl-3,4-dihydroxytetrahydrofuran-2-yl)methoxy)malonic Acid (39d). Proceeding as described in Method D for compound 39e above but substituting benzylamine with cyclopropylmethanamine provided the title compound 39d as a white solid. ¹H NMR (400 MHz, CD₃OD) δ ppm 8.14 (s, 1H), 7.18 (d, *J* = 6.9 Hz, 2H), 7.12–6.68 (m, 3H), 5.92 (d, *J* = 6.1 Hz, 1H), 4.58 (d, *J* = 6.1 Hz, 1H), 4.28 (t, *J* = 3.2 Hz, 1H), 3.98 (qd, *J* = 10.3, 3.2 Hz, 2H), 3.50–3.04 (m, 4H), 2.55 (s, 1H), 1.08 (m, 1H), 0.52 (m, 2H), 0.26 (m, 2H); LC/MS (ESI) [M + H]⁺ = 572.0.

2-Benzyl-2-(((2R,3S,4R,5R)-5-(2-chloro-6-((*R*)-1-phenylethyl)-amino)-9H-purin-9-yl)-3-ethynyl-3,4-dihydroxytetrahydrofuran-2-yl)methoxy)malonic Acid (39f**).**

Proceeding as described in Method D for compound **39e** above but substituting benzylamine with (*R*)-1-phenylethan-1-amine provided the title compound **39f** as a white solid. ¹H NMR (400 MHz, CDCl₃/CD₃OD = 5:1/v:v) δ ppm 8.25 (s, 1H), 7.44–7.27 (m, 4H), 7.23–6.94 (m, 6H), 5.91 (dd, *J* = 6.2, 1.7 Hz, 1H), 5.46 (d, *J* = 8.0 Hz, 1H), 4.58 (d, *J* = 6.2 Hz, 1H), 4.25 (t, *J* = 2.4 Hz, 1H), 3.98–3.83 (m, 2H), 3.32 (dd, *J* = 6.3, 1.7 Hz, 2H), 2.48 (d, *J* = 1.7 Hz, 1H), 1.59 (dd, *J* = 6.9, 1.7 Hz, 3H); LC/MS (ESI) [M + H]⁺ = 622.1.

2-Benzyl-2-(((2R,3S,4R,5R)-5-(2-chloro-6-((*S*)-1-phenylethyl)-amino)-9H-purin-9-yl)-3-ethynyl-3,4-dihydroxytetrahydrofuran-2-yl)methoxy)malonic Acid (39g**).**

Proceeding as described in Method D for compound **39e** above but substituting benzylamine with (*S*)-1-phenylethan-1-amine provided the title compound **39g** as a white solid. ¹H NMR (400 MHz, CDCl₃/CD₃OD = 5:1/v:v) δ ppm 8.11 (s, 1H), 7.40–7.28 (m, 4H), 7.23–6.93 (m, 6H), 5.90 (d, *J* = 5.8 Hz, 1H), 5.45 (s, 1H), 4.52 (d, *J* = 5.8 Hz, 1H), 4.35–4.22 (m, 1H), 3.99 (t, *J* = 2.4 Hz, 2H), 3.42–3.25 (m, 2H), 2.50 (s, 1H), 1.58 (d, *J* = 6.9 Hz, 3H); LC/MS (ESI) [M + H]⁺ = 622.2.

2-Benzyl-2-(((2R,3S,4R,5R)-5-(2-chloro-6-((2-hydroxyethyl)-amino)-9H-purin-9-yl)-3-ethynyl-3,4-dihydroxytetrahydrofuran-2-yl)methoxy)malonic Acid (39h**).**

Proceeding as described in Method D for compound **39e** above but substituting benzylamine with 2-aminoethanol provided the title compound **39h** as a white solid. ¹H-NMR (CD₃OD, 400 MHz) δ ppm 8.20 (s, 1H), 7.24–7.22 (m, 2H), 7.04–7.02 (m, 3H), 5.97 (d, *J* = 7.4Hz, 1H), 4.91 (d, *J* = 7.3Hz, 1H), 4.29 (t, *J* = 3.4Hz, 1H), 4.06–3.98 (m, 2H), 3.76–3.73 (m, 2H), 3.66–3.63 (m, 2H), 3.43–3.33 (m, 2H), 2.96 (s, 1H); LC/MS (ESI) [M + H]⁺ = 562.1.

2-Benzyl-2-(((2R,3S,4R,5R)-5-(2-chloro-6-(dimethylamino)-9H-purin-9-yl)-3-ethynyl-3,4-dihydroxytetrahydrofuran-2-yl)methoxy)malonic Acid (39i**).**

Proceeding as described in Method D for compound **39e** above but substituting benzylamine with dimethylamine provided the title compound **39i** as a white solid. ¹H NMR (400 MHz, CD₃OD) δ ppm 8.17 (s, 1H), 7.22 (dd, *J* = 7.5, 2.0 Hz, 2H), 7.05–6.89 (m, 3H), 5.98 (d, *J* = 7.2 Hz, 1H), 4.96 (d, *J* = 7.3 Hz, 1H), 4.28 (dd, *J* = 4.0, 2.9 Hz, 1H), 4.04 (qd, *J* = 10.2, 3.5 Hz, 2H), 3.55–3.31 (m, 8H), 2.95 (s, 1H); LC/MS (ESI) [M + H]⁺ = 546.0.

2-Benzyl-2-(((2R,3S,4R,5R)-5-(5-chloro-7-(isopropylamino)-3H-imidazo[4,5-*b*]pyridin-3-yl)-3-ethynyl-3,4-dihydroxytetrahydrofuran-2-yl)methoxy)malonic Acid (39k**) and 2-Benzyl-2-(((2R,3S,4R,5R)-5-(5-chloro-7-(dimethylamino)-3H-imidazo[4,5-*b*]pyridin-3-yl)-3-ethynyl-3,4-dihydroxytetrahydrofuran-2-yl)methoxy)malonic Acid (**39l**).**

Method E. To a solution of **23a** (500 mg, 0.91 mmol) in MeCN (6 mL) at 25 °C was added 5,7-dichloro-1*H*-imidazo[4,5-*b*]pyridine (223 mg, 1.18 mmol) followed by *N,O*-bis(trimethylsilyl)acetamide (BSA) (535 μL, 2.19 mmol). The resulting suspension was heated at 85 °C for 15 min as it became clear. The reaction mixture was cooled to 25 °C followed by the addition of TMSOTf (214 μL, 1.18 mmol) dropwise. The reaction mixture was then stirred at 85 °C for 3 h before it was cooled, quenched with cold saturated aq. NaHCO₃ solution, and then extracted with EtOAc (15 mL). The organic layer was washed with H₂O (20 mL) and brine, dried over Na₂SO₄, and concentrated. The crude residue was purified by flash column chromatography on silica gel (0–50% EtOAc in hexanes) to provide intermediate **38b** (122 mg, 20%) as a foam, which was used directly in the next step without further characterization. A sealed tube containing **38b** (80 mg, 0.12 mmol), isopropylamine (0.5 mL, 5.9 mmol), and Et₃N (1 mL) in anhydrous DMF (1 mL) was heated at 75 °C for 72 h before it was allowed to cool and partitioned with EtOAc (15 mL) and H₂O (5 mL). The organic layer was washed with H₂O (20 mL) and brine, dried over Na₂SO₄, and concentrated. The crude residue was purified by flash column chromatography on silica gel (0–50% EtOAc in hexanes) to provide two products: diethyl 2-benzyl-2-(((2R,3S,4R,5R)-5-(5-chloro-7-(isopropylamino)-3H-imidazo[4,5-*b*]pyridin-3-yl)-3-ethynyl-3,4-dihydroxytetrahydrofuran-2-yl)methoxy)malonate (10 mg, 14%) and diethyl 2-benzyl-2-(((2R,3S,4R,5R)-5-(5-

chloro-7-(dimethylamino)-3H-imidazo[4,5-*b*]pyridin-3-yl)-3-ethynyl-3,4-dihydroxytetrahydrofuran-2-yl)methoxy)malonate (21 mg, 31%) and both as foam. To a solution of intermediate diethyl 2-benzyl-2-(((2R,3S,4R,5R)-5-(5-chloro-7-(isopropylamino)-3H-imidazo[4,5-*b*]pyridin-3-yl)-3-ethynyl-3,4-dihydroxytetrahydrofuran-2-yl)methoxy)malonate (10 mg, 0.016 mmol) in a mixture of THF (3 mL) and H₂O (1 mL) at 25 °C was added LiOH·H₂O (10 mg, 0.24 mmol). The resulting mixture was stirred for 24 h before it was cooled to 0 °C and acidified to pH 6.5 with 1 N aq. HCl. The reaction mixture was then concentrated under reduced pressure. The crude residue was purified by preparative HPLC to provide the title compound **39k** (7 mg, 77%) as a white solid. ¹H NMR (300 MHz, CD₃OD) δ ppm 8.25 (s, 1H), 7.25–7.28 (m, 2H), 7.05 (m, 3H), 6.43 (s, 1H), 6.06–6.08 (d, *J* = 7.2 Hz, 1H), 4.95–4.98 (d, *J* = 7.0 Hz, 1H), 4.32 (s, 1H), 4.05–4.11 (m, 2H), 3.89–3.93 (m, 1H), 3.31–3.39 (m, 2H), 2.99 (s, 1H), 1.30–1.33 (m, 6H); LC/MS (ESI) [M + H]⁺ = 559.6.

To a solution of intermediate diethyl 2-benzyl-2-(((2R,3S,4R,5R)-5-(5-chloro-7-(dimethylamino)-3H-imidazo[4,5-*b*]pyridin-3-yl)-3-ethynyl-3,4-dihydroxytetrahydrofuran-2-yl)methoxy)malonate (21 mg, 0.035 mmol) from above in a mixture of THF (3 mL) and H₂O (1 mL) was added LiOH·H₂O (30 mg, 0.71 mmol). The resulting mixture was stirred at 25 °C for 24 h before it was cooled to 0 °C and acidified to pH 6.5 with 1 N aq. HCl solution. The reaction mixture was concentrated under reduced pressure. The crude residue was purified by preparative HPLC and dried by lyophilization to provide the title compound **39l** (12 mg, 63%) as a white solid. ¹H NMR (300 MHz, CD₃OD) δ ppm 8.68 (s, 1H), 7.21–7.24 (m, 2H), 6.99–7.03 (m, 3H), 6.49 (s, 1H), 6.15–6.17 (d, *J* = 7.1 Hz, 1H), 4.99–5.02 (d, *J* = 7.2 Hz, 1H), 4.35–4.37 (t, *J* = 3.1 Hz, 1H), 4.07–4.08 (m, 2H), 3.36–3.50 (m, 8H), 2.99 (s, 1H); LC/MS (ESI) [M + H]⁺ = 545.0.

2-Benzyl-2-(((2R,3S,4R,5R)-5-(2-chloro-6-(3-hydroxyazetidin-1-yl)-9H-purin-9-yl)-3-ethynyl-3,4-dihydroxytetrahydrofuran-2-yl)methoxy)malonic Acid (39j**).**

Proceeding as described in Method E for compound **39k** above but substituting 2,6-dichloroadenine with 5,7-dichloro-1*H*-imidazo[4,5-*b*]pyridine and benzylamine with azetidin-3-ol provided the title compound **39j** as a white solid. ¹H NMR (300 MHz, CD₃OD) δ ppm 8.29 (bs, 1H), 7.21–7.29 (m, 2H), 6.99–7.11 (m, 3H), 6.01 (d, *J* = 7.3 Hz, 1H), 5.01 (d, *J* = 7.3 Hz, 1H), 4.57–4.82 (m, 3H), 4.33 (t, *J* = 3.4 Hz, 1H), 4.14–4.27 (m, 2H), 4.07 (qd, *J* = 4.0, 2.9 Hz, 2H), 3.30–3.50 (m, 2H), 2.98 (s, 1H); LC/MS (ESI) [M + H]⁺ = 574.0.

2-Benzyl-2-(((2R,3S,4R,5R)-5-(2-chloro-6-(thiophen-2-yl)-9H-purin-9-yl)-3-ethynyl-3,4-dihydroxytetrahydrofuran-2-yl)methoxy)malonic Acid (41**).**

To a mixture of 2,6-dichloroadenine (800 mg, 4.23 mmol) in MeCN (5 mL) and H₂O (10 mL) at 20 °C under N₂ atmosphere were added 4,4,S,S-tetramethyl-2-(thiophen-2-yl)-1,3,2-dioxaborolane (800 mg, 3.81 mmol), Pd(OAc)₂ (48 mg, 0.21 mmol), Cs₂CO₃ (3.45 g, 10.58 mmol), and triphenylphosphine-3,3'-trisulfonic acid trisodium salt (601.50 mg, 1.06 mmol). The mixture was stirred at 110 °C for 3 h before it was allowed to cool, diluted with H₂O (10 mL), and partitioned with EtOAc (3 × 20 mL). The combined organic phase was washed with H₂O (2 × 10 mL), dried over Na₂SO₄, filtered, and concentrated. The crude product was triturated with a mixture of petroleum ether and EtOAc (v:v = 3:1) and left standing for 14 h. The precipitate was collected by filtration and dried to provide intermediate **40** (190 mg, 19%) as a yellow solid. ¹H NMR (400 MHz, DMSO-*d*₆) δ ppm 8.63 (s, 1H), 8.61 (dd, *J* = 3.8, 1.0 Hz, 1H), 7.97 (dd, *J* = 5.0, 1.2 Hz, 1H), 7.35 (dd, *J* = 5.0, 3.8 Hz, 1H); LC/MS (ESI) [M + H]⁺ = 236.9.

To a mixture of **40** (140 mg, 0.59 mmol) and **23a** (324 mg, 0.59 mmol) in MeCN (3 mL) under N₂ atmosphere at 0 °C was added DBU (267 μL, 1.77 mmol). The mixture was stirred at 0 °C for 10 min followed by dropwise addition of TMSOTf (481 μL, 2.66 mmol). The mixture was stirred for 30 min and then heated at 65 °C for 14 h. The reaction mixture was allowed to cool, diluted with saturated aq. NaHCO₃ (10 mL), and partitioned with EtOAc (3 × 20 mL). The combined organic phase was washed with brine (2 × 20 mL), dried over Na₂SO₄, filtered, and concentrated. The crude product was purified by preparative TLC (petroleum ether: EtOAc = 2:1) to

provide intermediate diethyl 2-benzyl-2-(((2R,3R,4R,5R)-3,4-diacetoxy-5-(2-chloro-6-(thiophen-2-yl)-9H-purin-9-yl)-3-ethynyltetrahydrofuran-2-yl)methoxy)-malonate (150 mg, 35%) as a white solid. ¹H NMR (400 MHz, DMSO-*d*₆) δ ppm 8.78 (s, 1H), 8.61 (dd, *J* = 3.8, 1.0 Hz, 1H), 8.04 (dd, *J* = 5.0, 1.0 Hz, 1H), 7.38 (dd, *J* = 4.9, 3.9 Hz, 1H), 7.13–7.19 (m, 2H), 7.02–7.12 (m, 3H), 6.27–6.31 (m, 1H), 6.21–6.25 (m, 1H), 4.70 (br d, *J* = 1.5 Hz, 1H), 4.10–4.17 (m, 4H), 4.03 (s, 1H), 2.06 (s, 3H), 1.12 (td, *J* = 7.1, 4.1 Hz, 1H); LC/MS (ESI) [M + H]⁺ = 725.0.

To a solution of the above intermediate (150 mg, 0.207 mmol) in THF (2 mL) was added a 2 M LiOH solution (2 mL). The mixture was stirred at 25 °C for 2 h before it was partitioned between EtOAc (10 mL) and water (10 mL). The aqueous phase was separated and adjusted to pH 2–3 with 2 N aq. HCl solution before it was extracted with EtOAc (40 mL). The organic layer was washed with brine (20 mL), dried over anhydrous Na₂SO₄, filtered, and concentrated. The crude product was purified by preparative HPLC to provide the title compound **41** (31.6 mg, 26%) as a white solid. ¹H NMR (400 MHz, DMSO-*d*₆) δ ppm 8.87 (s, 1H), 8.60 (dd, *J* = 3.8, 1.2 Hz, 1H), 8.02 (dd, *J* = 5.0, 1.0 Hz, 1H), 7.36 (dd, *J* = 4.9, 3.9 Hz, 1H), 7.16–7.28 (m, 2H), 6.93–7.10 (m, 3H), 6.31 (br s, 1H), 6.11 (br d, *J* = 6.0 Hz, 1H), 5.99 (d, *J* = 7.5 Hz, 1H), 4.88–4.97 (m, 1H), 4.23 (dd, *J* = 4.3, 2.8 Hz, 1H), 3.99 (br dd, *J* = 10.4, 4.4 Hz, 1H), 3.84 (br d, *J* = 8.5 Hz, 1H), 3.56 (s, 1H), 3.26 (s, 2H); LC/MS (ESI) [M + H]⁺ = 585.0.

2-((2R,3S,4R,5R)-5-(6-Amino-2-chloro-9H-purin-9-yl)-3-ethynyl-3,4-dihydroxytetrahydrofuran-2-yl)methoxy)-2-(4-(2-oxo-1,2-dihydropyridin-3-yl)benzyl)malonic Acid (47). To a solution of **14b** (12.59 g, 16.39 mmol) and 4-iodobenzyl bromide (48.67 g, 163.90 mmol) in DMF (120 mL) was added K₂CO₃ (33.98 g, 245.85 mmol). The reaction mixture was stirred at 20 °C for 16 h before it was diluted with water (200 mL) and extracted with EtOAc (3 × 200 mL). The combined organic layer was washed with water (400 mL) and brine (400 mL), dried over Na₂SO₄, filtered, and concentrated. The crude residue was purified by flash column chromatography on silica gel (15–40% EtOAc in petroleum ether) to give intermediate **45** (2.94 g, 18%) as a yellow solid. ¹H NMR (400 MHz, CDCl₃) δ ppm 8.62 (s, 1H), 7.54 (m, *J* = 8.2 Hz, 2H), 7.02 (m, *J* = 8.2 Hz, 2H), 6.30 (d, *J* = 6.0 Hz, 1H), 6.09 (d, *J* = 6.1 Hz, 1H), 4.63 (s, 1H), 4.08–4.35 (m, 5H), 3.37 (d, *J* = 17.4 Hz, 2H), 2.63 (s, 1H), 2.23 (s, 3H), 2.10 (s, 3H), 1.42–1.49 (m, 18H), 1.14–1.35 (m, 6H); LC/MS (ESI) [M + H]⁺ = 948.0.

To a solution of **45** (1.10 g, 1.12 mmol) and (2-oxo-1,2-dihydropyridin-3-yl)boronic acid (311 mg, 2.24 mmol) in dioxane (12 mL) and H₂O (4 mL) at 20 °C were added K₂CO₃ (463 mg, 3.35 mmol) and Pd(dppf)Cl₂ (81.78 mg, 0.112 mmol). The mixture was degassed with N₂ before it was heated at 80 °C under N₂ atmosphere for 1 h. The reaction mixture was allowed to cool, diluted with water (10 mL), and extracted with EtOAc (3 × 10 mL). The combined organic layer was washed with brine (30 mL), dried over Na₂SO₄, filtered, and concentrated. The crude residue was purified by flash column chromatography on silica gel (40–100% EtOAc in petroleum ether) to give intermediate diethyl 2-(((2R,3R,4R,5R)-3,4-diacetoxy-5-(6-N,N'-(bis-(*tert*-butoxy-carbonyl)amino)-2-chloro-9H-purin-9-yl)-3-ethynyltetrahydrofuran-2-yl)methoxy)-2-(4-(2-oxo-1,2-dihydropyridin-3-yl)benzyl)malonate (220 mg, 21%) as a yellow gum. LC/MS (ESI) [M + H]⁺ = 951.1.

To a solution of the above intermediate (180 mg, 0.169 mmol) in DCM (2.4 mL) at 20 °C was added TFA (0.6 mL, 8.10 mmol). The reaction was stirred for 2.5 h before it was quenched with saturated aq. NaHCO₃ (5 mL) and extracted with EtOAc (3 × 4 mL). The combined organic layer was concentrated. The crude residue was purified by preparative TLC (100% EtOAc) to give intermediate diethyl 2-(((2R,3R,4R,5R)-3,4-diacetoxy-5-(6-amino-2-chloro-9H-purin-9-yl)-3-ethynyltetrahydrofuran-2-yl)methoxy)-2-(4-(2-oxo-1,2-dihydropyridin-3-yl)benzyl)malonate (23 mg, 18%) as a yellow solid. LC/MS (ESI) [M + H]⁺ = 751.0.

To a solution of this resulting intermediate (23 mg, 0.031 mmol) in THF (2.5 mL) was added 1 M aq. LiOH (0.6 mL). The mixture was stirred at 20 °C for 4 h before it was acidified to pH 6 with 1 N aq. HCl and concentrated under reduced pressure. The crude residue was

purified by preparative HPLC and dried by lyophilization to give the title compound **47** (2.1 mg, 11%) as a white solid. ¹H NMR (400 MHz, CD₃OD) δ ppm 8.24 (s, 1H), 7.46 (dd, *J* = 6.9, 1.6 Hz, 1H), 7.28–7.34 (m, 5H), 6.39 (t, *J* = 6.7 Hz, 1H), 5.96 (d, *J* = 7.4 Hz, 1H), 4.77–4.84 (m, 1H), 4.29 (t, *J* = 2.9 Hz, 1H), 4.03 (d, *J* = 2.7 Hz, 2H), 3.38–3.51 (m, 2H), 3.04 (s, 1H); LC/MS (ESI) [M + H]⁺ = 611.0.

2-((2R,3S,4R,5R)-5-(6-Amino-2-chloro-9H-purin-9-yl)-3-ethynyl-3,4-dihydroxytetrahydrofuran-2-yl)methoxy)-2-(4-(2-oxopiperidin-1-yl)benzyl)malonic Acid (48). To a solution of **14b** (7.62 g, 4.92 mmol) in DMF (80 mL) was added K₂CO₃ (13.60 g, 98.40 mmol) at 20–25 °C. The reaction mixture was stirred for 0.5 h followed by the addition of 4-nitrobenzyl bromide (15.94 g, 73.80 mmol). The reaction mixture was stirred for 24 h before it was diluted with H₂O (300 mL) and extracted with EtOAc (3 × 60 mL). The combined organic layer was washed with brine (100 mL), dried over Na₂SO₄, filtered, and concentrated. The crude residue was passed through a short plug of silica gel (9–33% EtOAc in petroleum ether) to provide crude intermediate **46a** (2.36 g, 26%) as a gum, which was used in the next step without further purification.

To a solution of **46a** (2.26 g, 2.81 mmol) in EtOH (23 mL) at 0 °C was added iron powder (786 mg, 14.07 mmol) and a solution of NH₄Cl (151 mg, 2.81 mmol) in H₂O (8.5 mL). The reaction mixture was stirred at 50 °C for 4 h before it was allowed to cool. The reaction mixture was filtered through a pad of Celite, and the filtrate was concentrated. The crude residue was purified by flash column chromatography on silica gel (0–50% EtOAc in petroleum ether) to provide **46b** (280 mg, 13%) as a foam. ¹H NMR (400 MHz, CDCl₃) δ ppm 8.37 (s, 1H), 7.56 (s, 1H), 7.17–7.21 (d, *J* = 8.4 Hz, 2H), 7.08–7.13 (d, *J* = 8.8 Hz, 2H), 6.22 (d, *J* = 7.0 Hz, 1H), 6.03 (d, *J* = 7.0 Hz, 1H), 4.62–4.69 (m, 1H), 4.20–4.33 (m, 4H), 4.06 (m, 2H), 3.52–3.58 (m, 2H), 3.44 (br d, *J* = 19.3 Hz, 2H), 2.75 (s, 1H), 2.31 (m, 2H), 2.22 (s, 3H), 2.09 (s, 3H), 1.79–1.85 (m, 4H), 1.51 (s, 18H), 1.23–1.27 (m, 6H); LC/MS (ESI) [M + H]⁺ = 795.2.

To a solution of **46b** (140 mg, 0.18 mmol) in DCM (2 mL) at 0 °C was added TEA (147 μL, 1.06 mmol) followed by 5-chloropentanoyl chloride (24.9 μL, 0.192 mmol) dropwise. The mixture was stirred at 25 °C for 1 h before it was diluted with H₂O (20 mL) and extracted with DCM (20 mL). The organic phase was washed with brine (10 mL), dried over Na₂SO₄, filtered, and concentrated. The crude residue was purified by preparative TLC (petroleum ether: EtOAc = 1:1) to give intermediate **48a** (130 mg, 81%) as a yellow gum. ¹H NMR (400 MHz, CDCl₃) δ ppm 8.37 (s, 1H), 7.56 (s, 1H), 7.17–7.21 (d, *J* = 8.4 Hz, 2H), 7.08–7.13 (d, *J* = 8.8 Hz, 2H), 6.22 (d, *J* = 7.0 Hz, 1H), 6.03 (d, *J* = 7.0 Hz, 1H), 4.62–4.69 (m, 1H), 4.20–4.33 (m, 4H), 4.06 (m, 2H), 3.52–3.58 (m, 2H), 3.44 (br d, *J* = 19.3 Hz, 2H), 2.75 (s, 1H), 2.31 (m, 2H), 2.22 (s, 3H), 2.09 (s, 3H), 1.79–1.85 (m, 4H), 1.51 (s, 18H), 1.23–1.27 (m, 6H); LC/MS (ESI) [M + H]⁺ = 991.3.

To a solution of **48a** (104 mg, 0.117 mmol) in THF (2 mL) at 25 °C was added NaH (25.2 mg, 0.630 mmol, 60% in mineral oil). The mixture was stirred for 4 h before it was quenched with H₂O (1 mL). The reaction mixture was stirred at 20 °C for 14 h before it was partitioned between EtOAc (10 mL) and water (20 mL). The aqueous phase was acidified to pH 5–6 with 2 N aq. HCl solution before it was extracted with EtOAc (20 mL). The organic layer was washed with brine (10 mL), dried over anhydrous Na₂SO₄, filtered, and concentrated to give the crude intermediate **48b** (58 mg) as a colorless gum. LC/MS (ESI) [M + H]⁺ = 715.1.

To a mixture of crude **48b** (58 mg, 0.081 mmol) in DCM (500 μL) at 20 °C was added TFA (400 μL, 5.40 mmol). The mixture was stirred for 2 h before it was quenched with 2 N aq. LiOH (500 μL). The mixture was partitioned between EtOAc (10 mL) and water (10 mL). The organic layer was discarded and the aqueous phase was adjusted to pH 5–6 with 2 M aq. HCl solution before it was extracted with EtOAc (2 × 20 mL). The combined organic layer was washed with brine (5 mL), dried over anhydrous Na₂SO₄, filtered, and concentrated. The crude product was purified by preparative HPLC and lyophilized to give the title compound **48** (6.9 mg, 8% over 2 steps) as a white solid. ¹H NMR (400 MHz, DMSO-*d*₆) δ ppm 8.32 (s, 1H), 7.33 (d, *J* = 8.5 Hz, 2H), 6.98 (d, *J* = 8.3 Hz, 2H), 5.98 (d, *J* =

7.5 Hz, 1H), 4.79 (m, 1H), 4.28 (t, $J = 2.8$ Hz, 1H), 4.04 (br s, 2H), 3.39–3.54 (m, 4H), 3.05 (s, 1H), 2.43 (m, 2H), 1.88 (br t, $J = 2.9$ Hz, 4H); LC/MS (ESI) [M + H]⁺ = 615.3.

2-((2R,3S,4R,5R)-5-(6-Amino-2-chloro-9H-purin-9-yl)-3-ethynyl-3,4-dihydroxytetrahydrofuran-2-yl)methoxy)-2-(4-(2-oxotetrahydropyrimidin-1(2H)-yl)benzyl)malonic Acid (49). Proceeding as described for compound 48 above but substituting 5-chloropentanoyl chloride with 1-chloro-3-isocyanatopropane provided the title compound 49 as a white solid. ¹H NMR (400 MHz, CD₃OD) δ ppm 8.26 (s, 1H), 7.28 (d, $J = 8.3$ Hz, 2H), 7.00 (d, $J = 8.5$ Hz, 2H), 5.97 (d, $J = 7.2$ Hz, 1H), 4.91 (bs, 2H), 4.80 (br d, $J = 7.5$ Hz, 1H), 4.28 (s, 1H), 4.03 (bs, 2H), 3.38–3.57 (m, 4H), 3.30 (m, 2H), 3.05 (s, 1H), 1.89–2.09 (m, 2H); LC/MS (ESI) [M + H]⁺ = 616.2.

Recombinant CD73 Biochemical Assay. For measurements of soluble CD73 enzyme activity, recombinant CD73 was obtained from R&D Systems (Human: #5795-EN-010, Mouse: #4488-EN-010). Serial dilutions of test compounds were incubated with recombinant CD73 and AMP in reaction buffer (25 mM Tris HCl pH 7.5, 5 mM MgCl₂, 50 mM NaCl, 0.25 mM DTT, 0.005% Triton X-100). The final reaction volume was 25 μL, and the final concentrations of recombinant CD73 and AMP were 0.5 nM (changed to 0.05 nM for newer analogues with greater potency) and 50 μM, respectively. Reactions were allowed to proceed for 1 h at 37 °C before the addition of 100 μL of Malachite Green (Cell Signaling Technology #12776). After 5 min at room temperature, absorbance at 630 nm was determined on a microplate spectrophotometer. The concentration of inorganic phosphate was determined using a phosphate standard curve. The IC₅₀ data are reported as the average of at least two experiments.

CD73 Cell Surface Assay. The ability of compounds to inhibit endogenous, cell-bound CD73 enzyme activity was demonstrated using SK-MEL-28 cells, which express CD73 on their surface. The day before the experiment, 5000 cells were plated per well in a 96-well plate. The cells were washed twice with 200 μL of reaction buffer (20 mM HEPES, pH 7.4, 125 mM NaCl, 1 mM KCl, 2 mM MgCl₂, 10 mM glucose) to remove residual inorganic phosphate. After washing, assays contained serial dilutions of test compounds and 100 μM AMP in a total volume of 200 μL reaction buffer, with a final DMSO concentration ≤ 0.5%. After 30 min at room temperature, the supernatant was removed from the cells. A volume of 100 μL Malachite Green (Cell Signaling Technology, Cat. No. 12776) was added to 25 μL of supernatant. After 5 min at room temperature, absorbance at 630 nm was determined on a microplate spectrophotometer. The concentration of inorganic phosphate was determined using a phosphate standard curve to determine IC₅₀. The IC₅₀ data are reported as the average of at least two experiments.

Plasma CD73 Assay. For measurements of plasma CD73 enzyme activity, plasma was obtained either from normal healthy volunteers at Calithera or from BioIVT with sodium heparin as the anticoagulant. Serial dilutions of test compounds were added to the plasma. 100 μM TNAP inhibitor (EMD Millipore #613810) was added to all assays except for the mouse assay. ¹⁵N₅-AMP (25 μM) was added to obtain a final reaction volume of 50 μL with 45 μL being plasma. Reactions were allowed to proceed for 15 min at 37 °C (humans), 5 min at room temperature (mouse and rat), 10 min at room temperature (monkey), or 75 min at room temperature (dog). Reactions were quenched by the addition of 200 μL of ice-cold 30% acetonitrile, 56% methanol (human and mouse) or ice-cold 30% acetonitrile, 56% methanol, and 0.2% formic acid (monkey, dog, and rat). ¹⁵N₅-AMP and ¹⁵N₅-ADO in the supernatant were determined by LC/MS method. The IC₅₀ data are reported as the average of at least two experiments.

ASSOCIATED CONTENT

Supporting Information

The Supporting Information is available free of charge at <https://pubs.acs.org/doi/10.1021/acs.jmedchem.2c01287>.

Molecular formula strings ([CSV](#))

In vitro and *in vivo* study protocols and HPLC profile of compound 49 ([PDF](#))

AUTHOR INFORMATION

Corresponding Authors

Jim Li — *Calithera Biosciences, South San Francisco, California 94080, United States;* [orcid.org/0000-0001-8934-0682](#); Email: jimli808@gmail.com

Eric B. Sjogren — *Calithera Biosciences, South San Francisco, California 94080, United States;* Email: esjogren@calithera.com

Authors

Lijing Chen — *Calithera Biosciences, South San Francisco, California 94080, United States;* Present Address: PRA Health Sciences, Blue Bell, Pennsylvania 19422, United States

Roland J. Billedeau — *Calithera Biosciences, South San Francisco, California 94080, United States*

Timothy F. Stanton — *Calithera Biosciences, South San Francisco, California 94080, United States;* Present Address: Biomea Fusion, Redwood City, California 94063, United States.

John T. P. Chiang — *Calithera Biosciences, South San Francisco, California 94080, United States;* Present Address: Hexagon Bio, Menlo Park, California 94025, United States.

Clarissa C. Lee — *Calithera Biosciences, South San Francisco, California 94080, United States;* Present Address: 23andMe, Sunnyvale, California 94086, United States.

Weiqun Li — *Calithera Biosciences, South San Francisco, California 94080, United States;* Present Address: Biomea Fusion, Redwood City, California 94063, United States.

Susanne Steggerda — *Calithera Biosciences, South San Francisco, California 94080, United States;* Present Address: Erasca, San Diego, California 92121, United States.

Ethan Emberley — *Calithera Biosciences, South San Francisco, California 94080, United States;* Present Address: AbbVie, South San Francisco, California 94080, United States.

Matthew Gross — *Calithera Biosciences, South San Francisco, California 94080, United States*

Deepthi Bhupathi — *Calithera Biosciences, South San Francisco, California 94080, United States;* Present Address: Ideaya Biosciences, South San Francisco, California 94080, United States.

Xiaoying Che — *Wuxi AppTec, Shanghai 200131, China*

Jason Chen — *Calithera Biosciences, South San Francisco, California 94080, United States*

Rosalyn Dang — *Calithera Biosciences, South San Francisco, California 94080, United States;* Present Address: AbbVie, South San Francisco, California 94080, United States.

Tony Huang — *Calithera Biosciences, South San Francisco, California 94080, United States*

Yong Ma — *Calithera Biosciences, South San Francisco, California 94080, United States;* Present Address: Shanghai Hengrui Pharmaceuticals Co., Shanghai 200245, China.; [orcid.org/0000-0001-5901-5440](#)

Andrew MacKinnon — *Calithera Biosciences, South San Francisco, California 94080, United States*

Amani Makkouk — *Calithera Biosciences, South San Francisco, California 94080, United States;* Present

Address: AbbVie, South San Francisco, California 94080, United States.

Gisele Marguier — *Calithera Biosciences, South San Francisco, California 94080, United States; Present Address: Lyell Immunopharma, South San Francisco, California 94080, United States.*

Silinda Neou — *Calithera Biosciences, South San Francisco, California 94080, United States; Present*

Address: Gilmartin Group LLC., San Francisco, California 94939, United States.

Natalija Sotirovska — *Calithera Biosciences, South San Francisco, California 94080, United States*

Sandra Spurlock — *Calithera Biosciences, South San Francisco, California 94080, United States; Present Address: Johnson & Johnson, South San Francisco, California 94080, United States.*

Jing Zhang — *Calithera Biosciences, South San Francisco, California 94080, United States*

Winter Zhang — *Calithera Biosciences, South San Francisco, California 94080, United States*

Michael van Zandt — *NEDP, Branford, Connecticut 06405, United States; orcid.org/0000-0002-9624-5699*

Lin Yuan — *NEDP, Branford, Connecticut 06405, United States*

Jennifer Savoy — *NEDP, Branford, Connecticut 06405, United States*

Francesco Parlati — *Calithera Biosciences, South San Francisco, California 94080, United States*

Complete contact information is available at:

<https://pubs.acs.org/10.1021/acs.jmedchem.2c01287>

Notes

The authors declare no competing financial interest.

ACKNOWLEDGMENTS

The authors gratefully acknowledge all colleagues at Calithera Biosciences and collaborators at Wuxi AppTec and New England Discovery Partners (NEDP) who have supported this work.

ABBREVIATIONS USED

ADO, adenosine; AMP, adenosine monophosphate; AMPCP, adenosine 5'-(α,β -methylene)diphosphate; ATP, adenosine triphosphate; BID, twice-a-day dosing; BSA, *N,O*-bis(trimethylsilyl)acetamide; CD39, cluster of differentiation 39 or NTPDase 1; CD73, cluster of differentiation 73 or ecto-5'-nucleotidase; CL, clearance; CYP, cytochrome P450; DBU, 1,8-diazabicyclo[5.4.0]undec-7-ene; DC, dendritic cell; DCM, dichloromethane; DMF, *N,N*-dimethylamide; 4-DMAP, 4-(dimethylamino)pyridine; DMSO, dimethylsulfoxide; ENTPD2 and 3, ectonucleoside triphosphate diphosphohydrolase 2 and 3; EtOAc, ethyl acetate; HNSCC, head and neck squamous cell carcinoma; MDSC, myeloid-derived suppressor cell; MeCN, acetonitrile; MOMCl, methoxymethyl chloride; NK, natural killer; TAM, tumor-associated macrophage; TBAF, tetrabutylammonium fluoride; TBDMS, *t*-butyldimethylsilyl; TBDPS, *t*-butyldimethylsilyl; TEA, triethylamine; TFA, trifluoroacetic acid; THF, tetrahydrofuran; TME, tumor microenvironment; TMSOTf, trimethylsilyl trifluoromethanesulfonate; TNBC, triple-negative breast cancer

REFERENCES

- (1) Hanahan, D.; Weinberg, R. A. Hallmarks of Cancer: The Next Generation. *Cell* **2011**, *144*, 646–674.
- (2) Ladányi, A.; Tímár, J. Immunologic and Immunogenomic Aspects of Tumor Progression. *Semin. Cancer Biol.* **2020**, *60*, 249–261.
- (3) Taube, J. M.; Klein, L.; Brahmer, J.; Xu, H.; Pan, X.; Kim, J.; Chen, L.; Pardoll, D.; Topalian, S. L.; Anders, R. A. Association of PD-1, PDL-1 Ligands, and Other Features of the Tumor Immune Microenvironment with Response to Anti-PD-1 Therapy. *Clin. Cancer Res.* **2014**, *20*, 5064–5074.
- (4) Sharma, P.; Allison, J. P. The Future of Immune Checkpoint Therapy. *Science* **2015**, *348*, 56–61.
- (5) Allard, D.; Chrobak, P.; Allard, B.; Messaoudi, N.; Stagg, J. Targeting the CD73-adenosine Axis in Immuno-Oncology. *Immunol. Lett.* **2019**, *205*, 31–39.
- (6) Young, A.; Mittal, D.; Stagg, J.; Smyth, M. J. Targeting Cancer-derived Adenosine: New Therapeutic Approaches. *Cancer Discovery* **2014**, *4*, 879–888.
- (7) Ohta, A.; Ohta, A.; Madasu, M.; Kini, R.; Subramanian, M.; Goel, N.; Sitkovsky, M. A2A Adenosine Receptor May Allow Expansion of T Cells Lacking Effector Functions in Extracellular Adenosine-rich Microenvironments. *J. Immunol.* **2009**, *183*, 5487–5493.
- (8) Zarek, P. E.; Huang, C.-T.; Lutz, E. R.; Kowalski, J.; Horton, M. R.; Linden, J.; Drake, C. G.; Powell, J. D. A2A Receptor Signaling Promotes Peripheral Tolerance by Inducing T-cell Anergy and the Generation of Adaptive Regulatory T Cells. *Blood* **2008**, *111*, 251–259.
- (9) Vijayan, D.; Young, A.; Teng, M. W. L.; Smyth, M. J. Targeting Immunosuppressive Adenosine in Cancer. *Nat. Rev. Cancer* **2017**, *17*, 709–724.
- (10) Silva-Vilches, C.; Ring, S.; Mahnke, K. ATP and its Metabolite Adenosine as Regulators of Dendritic Cell Activity. *Front. Immunol.* **2018**, *9*, 2581.
- (11) Ernst, P. B.; Garrison, J. C.; Thompson, L. F. Much Ado about Adenosine: Adenosine Synthesis and Function in Regulatory T Cell Biology. *J. Immunol.* **2010**, *185*, 1993–1998.
- (12) Zimmermann, H. 5'-Nucleotidase: Molecular Structure and Functional Aspects. *Biochem. J.* **1992**, *285*, 345–365.
- (13) Sträter, N. Ecto-5'-nucleotidase: Structure Function Relationships. *Purinergic Signalling* **2006**, *2*, No. 343.
- (14) Antonioli, L.; Pacher, P.; Vizi, S.; Haskó, G. CD39 and CD73 in Immunity and Inflammation. *Trends Mol. Med.* **2013**, *19*, 355–367.
- (15) Allard, B.; Longhi, M. S.; Robson, S. C.; Stagg, J. The Ectonucleotidases CD39 and CD73: Novel Checkpoint Inhibitor Targets. *Immunol. Rev.* **2017**, *276*, 121–144.
- (16) Nooshabadi, V. T.; Arab, S. Targeting Tumor-derived Exosomes Expressing CD73: New Opportunities in the Pathogenesis and Treatment of Cancer. *Curr. Mol. Med.* **2021**, *21*, 476–483.
- (17) Leclerc, B. G.; Charlebois, R.; Chouinard, G.; Allard, B.; Pommy, S.; Saad, F.; Stagg, J. CD73 Expression is An Independent Prognostic Factor in Prostate Cancer. *Clin. Cancer Res.* **2016**, *22*, 158–166.
- (18) Jiang, T.; Xu, X.; Qiao, M.; Li, X.; Zhao, C.; Zhou, F.; Gao, G.; Wu, F.; Chen, X.; Su, C.; Ren, S.; Zhai, C.; Zhou, C. Comprehensive Evaluation of NTSE/CD73 Expression and its Prognostic Significance in Distinct Types of Cancers. *BMC Cancer* **2018**, *18*, 267.
- (19) Allard, B.; Turcotte, M.; Stagg, J. Targeting CD73 and Downstream Adenosine Receptor Signaling in Triple-negative Breast Cancer. *Expert Opin. Ther. Targets* **2014**, *18*, 863–881.
- (20) Chen, Q.; Pu, N.; Yin, H.; Zhang, J.; Zhao, G.; Lou, W.; Wu, W. CD73 Acts as a Prognostic Biomarker and Promotes Progression and Immune Escape in Pancreatic Cancer. *J. Cell Mol. Med.* **2020**, *24*, 8674–8686.
- (21) Messaoudi, N.; Cousineau, I.; Arslanian, E.; Henault, D.; Stephen, D.; Vandebroucke-Menu, F.; Dagenais, M.; Létourneau, R.; Plasse, M.; Roy, A.; Lapointe, R.; Ysebaert, D.; Trudel, D.; Soucy, G.; Stagg, J.; Turcotte, S. Prognostic Value of CD73 Expression in

- Resected Colorectal Cancer Liver Metastasis. *Oncoimmunology* **2020**, 9, No. e1746138.
- (22) Monteiro, I.; Vigano, S.; Faouzi, M.; Treilleux, I.; Michelin, O.; Ménétrier-Caux, C.; Caux, C.; Romero, P.; Leval, L. D. CD73 Expression and Clinical Significance in Human Metastatic Melanoma. *Oncotarget* **2018**, 9, 26659–26669.
- (23) Turcotte, M.; Spring, K.; Pommey, S.; Chouinard, G.; Cousineau, I.; George, J.; Chen, G. M.; Gendoo, D. M. A.; Kains, B.; Karn, T.; Rahimi, K.; Page, C. L.; Provencher, D.; Mes-Masson, A.-M.; Stagg, J. CD73 is Associated with Poor Prognosis in High-grade Serous Ovarian Cancer. *Cancer Res.* **2015**, 75, 4494–4503.
- (24) Harvey, J. B.; Phan, L. H.; Villarreal, O. E.; Bowser, J. L. CD73's Potential as an Immunotherapy Target in Gastrointestinal Cancers. *Front. Immunol.* **2020**, 11, 508.
- (25) Bertoni, A. P. S.; Braccob, P. A.; de Campos, R. P.; Lutz, B. S.; Assis-Brasild, B. M.; de Souza Meyer, E. L.; Saffi, J.; Braganhol, E.; Furlanetto, T. W.; Wink, M. R. Activity of Ecto-5'-nucleotidase (NTSE/CD73) is Increased in Papillary Thyroid Carcinoma and Its Expression is Associated with Metastatic Lymph Nodes. *Mol. Cell. Endocrinol.* **2019**, 479, 54–60.
- (26) Knapp, K.; Zebisch, M.; Pippel, J.; El-Tayeb, A.; Müller, C. E.; Sträter, N. Crystal Structure of the Human Ecto-5'-Nucleotidase (CD73): Insights into the Regulation of Purinergic Signaling. *Structure* **2012**, 20, 2161–2173.
- (27) Hay, C. M.; Sult, E.; Huang, Q.; Mulgrew, K.; Fuhrmann, S. R.; McGlinchey, K. A.; Hammond, S. A.; Rothstein, R.; Rios-Doria, J.; Poon, E.; Holowecyk, N.; Durham, N. M.; Leow, C. C.; Diedrich, G.; Damschroder, M.; Herbst, R.; Hollingsworth, R. E.; Sachsenmeier, K. F. Targeting CD73 in the Tumor Microenvironment with MEDI9447. *OncoImmunology* **2016**, 5, No. e1208875.
- (28) Siu, L. L.; Burris, H.; Le, D. T.; Hollebecque, A.; Steeghs, N.; Delord, J.-P.; Hilton, J.; Barnhart, B.; Segal, E.; Sanghani, K.; Klippen, A.; Hedvat, C.; Hilt, E.; Donovan, M.; Gipson, A.; Basciano, P.; Postelnek, J.; Zhao, Y.; Perez, R. P.; Carvajal, R. D. Abstract CT180: Preliminary Phase 1 Profile of BMS-986179, an Anti-CD73 Antibody, in Combination with Nivolumab in Patients with Advanced Solid Tumors. *Cancer Res.* **2018**, 78, No. CT180.
- (29) Cacatian, S.; Claremon, D. A.; Jia, L.; Morels-Ramos, A.; Singh, S. B.; Venkatraman, S.; Xu, Z.; Zheng, Y. Purine Derivatives as CD73 Inhibitors for the Treatment of Cancer. WO2015/164573A1, 2015.
- (30) Chen, L.; Li, J.; Sjogren, E. B.; Billedieu, R. J. Ectonucleotidase Inhibitors and Methods of Use Thereof. WO2018/49145A1, 2018.
- (31) Billedieu, R. J.; Li, J.; Chen, L. Ectonucleotidase Inhibitors and Methods of Use Thereof. WO2018/119284A1, 2018.
- (32) Bhattacharai, S.; Freundlieb, M.; Pippel, J.; Meyer, A.; Abdelrahman, A.; Fiene, A.; Lee, S.-Y.; Zimmermann, H.; Yegutkin, G. G.; Sträter, N.; El-Tayeb, A.; Müller, C. E. α,β -Methylene-ADP (AOPCP) Derivatives and Analogs: Development of Potent and Selective Ecto-5'-nucleotidase (CD73) Inhibitors. *J. Med. Chem.* **2015**, 58, 6248–6263.
- (33) Bhattacharai, S.; Pippel, J.; Meyer, A.; Freundlieb, M.; Schmies, C.; Abdelrahman, A.; Fiene, A.; Lee, S.-Y.; Zimmermann, H.; El-Tayeb, A.; Yegutkin, G. G.; Sträter, N.; Müller, C. E. X-Ray Co-crystal Structure Guides the Way to Subnanomolar Competitive Ecto-5'-nucleotidase (CD73) Inhibitors for Cancer Immunotherapy. *Adv. Ther.* **2019**, 2, No. 1900075.
- (34) Junker, A.; Renn, C.; Dobelmann, C.; Namasivayam, V.; Jain, S.; Losenkova, K.; Irjala, H.; Duca, S.; Balasubramanian, R.; Chakraborty, S.; Börgel, F.; Zimmermann, H.; Yegutkin, G. G.; Müller, C. E.; Jacobson, K. A. Structure–activity Relationship of Purine and Pyrimidine Nucleotides as Ecto-5'-nucleotidase (CD73) Inhibitors. *J. Med. Chem.* **2019**, 62, 3677–3695.
- (35) Lawson, K. V.; Kalisiak, J.; Lindsey, E. A.; Newcomb, E. T.; Reddy Leeti, M.; Debien, L.; Rosen, B. R.; Miles, D. H.; Sharif, E. U.; Jeffrey, J. L.; Tan, J. B. L.; Chen, A.; Zhao, S.; Xu, G.; Fu, L.; Jin, L.; Park, T. W.; Berry, W.; Moschütz, S.; Scaletti, E.; Sträter, N.; Walker, N. P.; Young, S. W.; Walters, M. J.; Schindler, U.; Powers, J. P. Discovery of AB680: A Potent and Selective Inhibitor of CD73. *J. Med. Chem.* **2020**, 63, 11448–11468.
- (36) Bowman, C. E.; Silva, R. G. d.; Pham, A.; Young, S. W. An Exceptionally Potent Inhibitor of Human CD73. *Biochemistry* **2019**, 58, 3331–3334.
- (37) Sharif, E. U.; Kalisiak, J.; Lawson, K. V.; Miles, D. H.; Newcomb, E.; Lindsey, E. A.; Rosen, B. R.; Debien, L. P. P.; Chen, A.; Zhao, X.; Young, S. W.; Walker, N. P.; Sträter, N.; Scaletti, E. R.; Jin, L.; Xu, G.; Leeti, M. R.; Powers, J. P. Discovery of Potent and Selective Methylenephosphonic Acid CD73 Inhibitors. *J. Med. Chem.* **2021**, 64, 845–860.
- (38) Du, X.; Moore, J.; Blank, B. R.; Eksterowicz, J.; Sutimantanapi, D.; Yuen, N.; Metzger, T.; Chan, B.; Huang, T.; Chen, X.; Chen, Y.; Duong, F.; Kong, W.; Chang, J. H.; Sun, J.; Zavorotinskaya, T.; Ye, Q.; Juntila, M. R.; Ndubaku, C.; Friedman, L. S.; Fantin, V. R.; Sun, D. Orally Bioavailable Small-Molecule CD73 Inhibitor (OP-5244) Reverses Immunosuppression through Blockade of Adenosine Production. *J. Med. Chem.* **2020**, 63, 10433–10459.
- (39) Beatty, J. W.; Lindsey, E. A.; Thomas-Tran, R.; Debien, L.; Mandal, D.; Jeffrey, J. L.; Tran, A. T.; Fournier, J.; Jacob, S. D.; Yan, X.; Drew, S. L.; Ginn, E.; Chen, A.; Pham, A. T.; Zhao, S.; Jin, L.; Young, S. W.; Walker, N. P.; Reddy Leeti, M.; Moschütz, S.; Sträter, N.; Powers, J. P.; Lawson, K. V. Discovery of Potent and Selective Non-Nucleotide Small Molecule Inhibitors of CD73. *J. Med. Chem.* **2020**, 63, 3935–3955.
- (40) Adams, J. L.; Ator, L. E.; Duffy, K. J.; Graybill, T. L.; Kiesow, T. J.; Lian, Y.; Moore, M. L.; Ralph, J. M.; Ridgers, L. H. Benzothiadiazine Compounds. WO2017/098421A1, 2017.
- (41) Dally, R. D.; Garcia Paredes, M. C.; Heinz, L. J., II; Howell, J. M.; Njoroge, F. G.; Wang, Y.; Zhao, G. CD73 Inhibitors. WO2019/168744A1, 2019.
- (42) AB680 was reported to be highly plasma protein bound with low free fraction (fu): 0.42% (human), 0.89% (mouse) and 0.17% (rat) according to ref 35.
- (43) Bloomfield, V.; Crothers, D.; Tinoco, I. *Nucleic Acids: Structures, Properties, and Functions*; University Science Books, 2000; pp 19–25.
- (44) Foloppe, N.; MacKerell, A. D. Conformational Properties of the Deoxyribose and Ribose Moieties of Nucleic Acids: A Quantum Mechanical Study. *J. Phys. Chem. B* **1998**, 102, 6669–6678.
- (45) Talele, T. T. Acetylene Group, Friend or Foe in Medicinal Chemistry. *J. Med. Chem.* **2020**, 63, 5625–5663.
- (46) Allard, B.; Pommey, S.; Smyth, M. J.; Stagg, J. Targeting CD73 Enhances the Antitumor Activity of Anti-PD-1 and Anti-CTLA-4 mAbs. *Clin. Cancer Res.* **2013**, 19, 5626–5635.
- (47) Vigano, S.; Alatzoglou, D.; Irving, M.; Ménétrier-Caux, C.; Caux, C.; Romero, P.; Coukos, G. Targeting Adenosine in Cancer Immunotherapy to Enhance T-Cell Function. *Front. Immunol.* **2019**, 10, 925–955.
- (48) Roh, M.; Wainwright, D. A.; Wu, J. D.; Wan, Y.; Zhang, B. Targeting CD73 to Augment Cancer Immunotherapy. *Curr. Opin. Pharmacol.* **2020**, 53, 66–76.
- (49) Galluzzi, L.; Buqué, A.; Kepp, O.; Zitvogel, L.; Kroemer, G. Immunogenic Cell Death in Cancer and Infectious Diseases. *Nat. Rev. Immunol.* **2017**, 17, 97–111.
- (50) Loi, S.; Pommey, S.; Haibe-Kains, B.; Beavisd, P. A.; Darcy, P. K.; Smyth, M. J.; Stagg, J. CD73 Promotes Anthracycline Resistance and Poor Prognosis in Triple Negative Breast Cancer. *Proc. Natl. Acad. Sci. U.S.A.* **2013**, 110, 11091–11096.
- (51) Nevedomskaya, E.; Perryman, R.; Solanki, S.; Syed, N.; Mayboroda, O. A.; Keun, H. C. A Systems Oncology Approach Identifies NTSE as a Key Metabolic Regulator in Tumor Cells and Modulator of Platinum Sensitivity. *J. Proteome Res.* **2016**, 15, 280–290.
- (52) Chun, M. W.; Kim, M. J.; Jo, U. H.; Kim, J. H.; Kim, H.-D.; Jeong, L. S. Synthesis of Novel D- and L-3'-Deoxy-3'-C-hydroxymethyl Nucleoside with Exocyclic Methyleno as Potential Ribonucleotide Reductase Inhibitor. *Nucleosides, Nucleotides Nucleic Acids* **2001**, 20, 703–706.
- (53) Vorbrüggen, H.; Ruh-Pohlenz, C. Synthesis of Nucleosides. In *Organic Reactions*; Wiley: Hoboken, NJ, 2000; p 55.

- (54) Parr, I. B.; Horenstein, B. A. New Electronic Analogs of the Sialyl Cation: *N*-Functionalized 4-Acetamido-2,4-dihydroxypiperidines. Inhibition of Bacterial Sialidases. *J. Org. Chem.* 1997, 62, 7489–7494.

□ Recommended by ACS

Discovery of a New-Generation S-Adenosylmethionine-Noncompetitive Covalent Inhibitor Targeting the Lysine Methyltransferase Enhancer of Zeste Homologue 2

Yi Zhang, Yuanxiang Wang, *et al.*

MAY 19, 2023

JOURNAL OF MEDICINAL CHEMISTRY

READ ▶

Discovery of CZS-241: A Potent, Selective, and Orally Available Polo-Like Kinase 4 Inhibitor for the Treatment of Chronic Myeloid Leukemia

Yin Sun, Maosheng Cheng, *et al.*

FEBRUARY 03, 2023

JOURNAL OF MEDICINAL CHEMISTRY

READ ▶

Discovery of a Potent and Selective CCR8 Small Molecular Antagonist IPG7236 for the Treatment of Cancer

Yong Wu, Guo-Huang Fan, *et al.*

MARCH 29, 2023

JOURNAL OF MEDICINAL CHEMISTRY

READ ▶

Discovery of GDC-0077 (Inavolisib), a Highly Selective Inhibitor and Degrader of Mutant PI3K α

Emily J. Hanan, Steven T. Staben, *et al.*

DECEMBER 01, 2022

JOURNAL OF MEDICINAL CHEMISTRY

READ ▶

[Get More Suggestions >](#)